

# **Investigation of Electro Discharge Machining of Aerospace Alloys**



**By**

**Shahid Hussain**

**Reg# 00000204203**

**Session: 2017-2021**

Supervised by

**Prof. Dr. Khalid Mahmood**

A Thesis Submitted to Department of Mechanical Engineering for Advance  
study in Machining in partial fulfillment of the requirements for the degree  
of

**Master of Science in  
(Mechanical Engineering)**

Mechanical Engineering Department  
College of Electrical & Mechanical Engineering (CEME)  
National University of Sciences and Technology,

**Rawalpindi**

**September, 2021**

# **Investigation of Electro Discharge Machining of Aerospace Alloys**

Author

Shahid Hussain

Regn Number

204203

A thesis submitted in partial fulfillment of the requirements for the degree

of

MS Mechanical Engineering

Thesis Supervisor:

Dr. Khalid Mahmood

Thesis Supervisor's Signature;

---

MECHANICAL ENGINEERING DEPARTMENT  
COLLEGE OF ELECTRICAL & MECHANICAL ENGINEERING  
(CEME)

NATIONAL UNIVERSITY OF SCIENCES AND TECHNOLOGY,

RAWALPINDI

AUGUST 2021

# Thesis Acceptance Certificate

Certified that final copy of MS/MPhil Thesis Written by Mr. Shahid Hussain (Registration No: 00000204203), of College of Electrical & Mechanical Engineering (School/College/Institute) has been vetted by undersigned, found complete in all respects as per NUST Statutes/ Regulations, is free of plagiarism, errors and mistakes and is accepted as partial fulfillment for award of MS/MPhil Degree. It is further certified that necessary amendments as pointed out by GEC members of the scholar have also been incorporated in the said thesis.

Signature: \_\_\_\_\_

Name of the supervisor: Dr. Khalid Mahmood

Date: \_\_\_\_\_

Signature (HOD): \_\_\_\_\_

Date: \_\_\_\_\_

Signature (Principle): \_\_\_\_\_

Date: \_\_\_\_\_

**National University of Science and Technology**  
**MASTER THESIS WORK**

We hereby recommended that the dissertation prepared under our supervision by **Shahid Hussain** (00000204203) titled: “**Investigation of electro discharge machining of aerospace alloys**” be accepted in partial fulfillment of the requirements for the MS Mechanical Engineering Degree with (\_\_\_) grade.

**Examination Committee Members**

1. Name: Dr. Syed Hussain Imran Signature: \_\_\_\_\_

2. Name: Dr. Hassan Aftaab Signature: \_\_\_\_\_

Supervisor Name: Dr. Khalid Mahmood Signature: \_\_\_\_\_

Date: \_\_\_\_\_

\_\_\_\_\_

Date: \_\_\_\_\_

Head of Department

**COUNTERSIGNED**

\_\_\_\_\_

Date: \_\_\_\_\_

Dean/Principal

# Declaration

I certified that this research work titled “**Investigation of Electro Discharge Machining of Aerospace Alloys**” is my own work. The work has not been presented elsewhere for assessment. The material that has been used from other sources it has been properly acknowledge/referred.

---

Shahid Hussain

(00000204203)

# Proposed Certificate for Plagiarism

It is certified that MS Thesis Titled “**Investigation of electro discharge machining of aerospace alloys**” by **Shahid Hussain (204203)** has been examined by us.

We undertake the follows:

- a. Thesis has significant new work/knowledge as compared already published or are under consideration to be published elsewhere. No sentence, equation, diagram, table, paragraph or section has been copied verbatim from previous work unless it is placed under quotation marks and duly referenced.
- b. The work presented is original and own work of the author (i.e. there is no plagiarism). No ideas, processes, results or words of others have been presented as Author own work.
- c. There is no fabrication of data or results which have been compiled/analyzed.
- d. There is no falsification by manipulating research materials, equipment or processes, or changing or omitting data or results such that the research is not accurately represented in the research record.
- e. The thesis has been checked using TURNITIN (copy of originality report attached) and found within limits as per HEC plagiarism Policy and instructions issued from time to time

**Name & Signature of Supervisor**

**Dr. Khalid Mahmood**

Signature: \_\_\_\_\_

# Copyright Statement

Copyright in text of this thesis rests with the student author. Copies (by any process) either in full, or of extracts, may be made only in accordance with instructions given by the author and lodged in the Library of CEME, NUST. Details may be obtained by the Librarian. This page must form part of any such copies made. Further copies (by any process) may not be made without the permission (in writing) of the author.

The ownership of any intellectual property rights which may be described in this thesis is vested in CEME, NUST, subject to any prior agreement to the contrary, and may not be made available for use by third parties without the written permission of CEME, NUST, which will prescribe the terms and conditions of any such agreement.

Further information on the conditions under which disclosures and exploitation may take place is available from the Library of CEME, NUST Rawalpindi.

# Acknowledgement

This Thesis work has been done at College of Electrical & Mechanical Engineering (CEME) at NUST, Rawalpindi, under the project “*Investigation of electro discharge machining of aerospace alloys*” and is submitted in partial fulfillment of the requirements for the degree of Master of Science program in Mechanical Engineering at CEME, NUST University.



# Dedication

*To my Beloved Parents,*

*Without whom none of my success  
would have been possible*

*&*

*To my Respected Teachers,*

*Who acted like compass  
that activated the magnets of  
curiosity, knowledge and wisdom in me*

# Abstract

Titanium and nickel-based alloys are materials of choice for many applications. Their high strength and low density make them a suitable candidate for aerospace applications. Besides these properties, these alloys exhibit remarkable corrosion resistance and biocompatibility. These properties make them suitable candidate for orthopedics implants. Whereas the reactivity and heat resistance of these alloys renders them difficult to machine. One of the known substitutes to the traditional cutting method is wire electrical discharge machining which is commonly being used nowadays to process materials that are tough to be machined on conventional machines being hard in nature, such as aerospace alloys. Based on previous research involving the effect of input variables on the output variables, this research aims to identify best machine setup for a quality product. Starting with Peak current, Wire feed rate, Pulse on time and Pulse off time as input parameters, and their effect on surface roughness and kerf width has been studied. Influence of these process conditions of the wire electro-discharge machining on grains distortion analyzed through SEM analysis results. Peak current and pulse on time are significant factors for kerf width of Inconel 600, for the kerf width of titanium alloy peak current and wire feed rate are found significant factors. For smoother surface, higher feed rate and intermediate current values are preferable for Inconel 600, however for titanium alloy high pulse off time and intermediate values of peak current are desirable for smooth surface finish. More grain distortion was observed for samples with greater surface roughness.

**Keywords:** Electrical discharge machining, aerospace alloys, kerf width, surface roughness, grain distortion, SEM analysis.

# Table of Contents

Abstract .....	x
Table of Contents .....	xi
List of figures .....	xv
List of tables .....	xvii
Nomenclature .....	xix
CHAPTER 1.....	1
Introduction: .....	1
1.1 Thesis Design.....	1
1.2 Problem Statement .....	2
1.3 Research Objectives .....	2
CHAPTER 2.....	3
2.1 Literature Review: .....	3
2.2) Aerospace Alloys:.....	6
2.1.1) Titanium Alloys.....	6
2.1.2) Nickel Alloys .....	7
2.2) Wire Electrical Discharge Machining .....	8
2.2.1) Introduction .....	8
2.2.2) Working Principle.....	8
2.2.3) Main Components and Working.....	9
2.2.4) Wire Used .....	11
2.2.5) Advantages of WEDM .....	11
2.2.6) Applications of Wire electro Discharge Machining.....	12
2.2.7) Limitations of Wire Electro Discharge Machining.....	12
2.2.8) WEDM process parameters .....	12
2.3) Flow Chart for Experimentation .....	13
CHAPTER 3.....	14
EXPERIMENTATION AND CHARACTERIZATION TECHNIQUES .....	14
3.1) List of Equipment .....	14
3.2) Work Piece Material .....	14

3.3) EDS Analysis .....	14
3.3.1) Inconel 600.....	15
3.3.2) Titanium Grade V .....	15
3.4) Mechanical Properties .....	16
3.4.1) Vickers Hardness Test .....	16
3.4.2) Rockwell Hardness Test .....	16
3.4.3) Test Results .....	17
3.5) Wire Electro Discharge Machine.....	17
3.6) Wire Used .....	18
3.7) Selection of Process Parameters .....	18
3.8) Taguchi Methodology and Design of experiments .....	19
3.9) Methodology.....	21
3.10) Measurement of Response Parameters .....	22
3.10.1) Kerf Width ( $\mu\text{m}$ ) .....	22
3.10.2) Surface Roughness ( $\mu\text{m}$ ) .....	24
3.11) Analysis of variance (ANOVA) .....	26
3.11.1) Regression Analysis.....	26
3.11.2) Confirmation of test.....	26
3.12) SEM Analysis .....	27
3.12.1) Sample Preparation .....	27
3.12.2) Sample Cutting.....	27
3.12.3) Sample Mounting.....	27
3.12.4) Sample Grinding.....	28
3.12.5) Sample Polishing .....	29
3.13) XRD Analysis.....	30
CHAPTER 4.....	31
Wire Electro Discharge Machining of Inconel 600.....	31
4.1) Kerf width results.....	31
4.1.1) Response Table for Data Means .....	32
4.1.2) Analysis of Variance .....	32
4.1.3) Regression Equation .....	33
4.1.4) Model Summary.....	33

4.1.6) Data Means Plot.....	34
4.2) Kerf Width Analysis.....	34
4.2.1) Peak Current (C).....	34
4.2.2) Pulse of time (Poff) .....	35
4.2.3) Pulse on time (Pon).....	35
4.2.4) Wire Feed Rate (WFR).....	35
4.3) Optimal Process Parameters.....	35
4.3.1) Confirmation Test .....	35
4.4) Surface Roughness Results .....	36
4.4.1) Response Table for Data Means .....	36
4.4.2) Analysis of Variance .....	37
4.4.3) Regression Equation .....	38
4.4.4) Model summary.....	38
4.4.6) Data Means Plot.....	38
4.5) Surface Roughness Analysis.....	39
4.5.1) Peak Current (C).....	39
4.5.2) Pulse off time (Poff) .....	39
4.5.3) Pulse on time (Pon).....	40
4.5.4) Wire Feed Rate (WFR).....	40
4.6) Optimal Process Parameters.....	40
4.6.1) Confirmation Test Result .....	40
4.7) XRD Analysis.....	41
4.8) SEM Analysis for Grain Distortion Measurement .....	41
CHAPTER 5.....	43
Wire Electro Discharge Machining of Titanium Grade V .....	43
5.1.1) Response Table for Data Means .....	44
5.1.2) Analysis of Variance .....	44
5.1.3) Regression Equation .....	45
5.1.4) Model Summary.....	45
5.1.6) Data Means Plot.....	45
5.2) Kerf Width Analysis.....	46
5.2.1) Peak current (C) .....	46

5.2.2) Pulse off time (Poff) .....	46
5.2.3) Pulse on time (Pon) .....	46
5.2.4) Wire Feed Rate (WFR) .....	46
5.3) Optimal Process Parameters .....	46
5.3.1) Confirmation Test .....	47
5.4) Surface Roughness Results .....	47
5.4.1) Response Table for Data Means .....	48
5.4.2) Analysis of Variance .....	48
5.4.3) Regression Equation .....	49
5.4.4) Model Summary .....	49
5.4.6) Main Effect Plot for Data Means .....	49
5.5) Surface Roughness Analysis .....	50
5.5.1) Peak Current (C) .....	50
5.5.2) Pulse off time (Poff) .....	50
5.5.3) Pulse on time (Pon) .....	51
5.5.4) Wire feed rate (WFR) .....	51
5.6) Optimal Process Parameters .....	51
5.6.1) Confirmation Test Result .....	51
5.7) XRD Analysis .....	52
5.8) SEM Analysis for Grain Distortion Measurement .....	52
CHAPTER 6 .....	54
CONCLUSIONS AND RECOMMENDATIONS .....	54
6.1) Conclusions .....	54
6.2) Recommendations .....	55
REFERENCES .....	56

# List of figures

Figure 1.1 Layout for project design	2
Figure 2.1 Turbofan engine of Rolls Royce showing main Parts comprising titanium and nickel alloys	6
Figure 2.2 working principle of wire electrical discharge machine	9
Figure 2.3 Components of WEDM Machine	9
Figure 2.4 Flow chart for experimentation	13
Figure 3.1 EDS spectrum of Inconel 600	15
Figure 3.2 EDS spectrum of Titanium Grade V	16
Figure 3.3 Wire electrical discharge machine	17
Figure 3.4 Samples after WEDM	22
Figure 3.5 WEDM Cut and Kerf	23
Figure 3.6 Metallurgical Microscope	23
Figure 3.7 Images from optical microscope	24
Figure 3.8 Optical Profilometer	25
Figure 3.9 Surface roughness profile of Sample T-6/2	25
Figure 3.10 Machined sample before mounting	27
Figure 3.11 Hydro-press mounting machine	28
Figure 3.12 Mounted Sample	28
Figure 3.13 Automatic grinding and Polishing Machine	29
Figure 4.1 Main effect plots for data means for kerf width	34
Figure 4.2 Main effect plot for data means for surface roughness	40
Figure 4.3 XRD graph for WEDM samples	41
Figure 4.4 Grain distortion of machined surface	42

Figure 5.1 Main effect plots for data means for kerf width	45
Figure 5.2 Main effect plot for data means for surface roughness	50
Figure 5.3 XRD graph for WEDM samples	52
Figure 5.4 Grain distortion of machined surface	53



# List of tables

Table 2.1 Process parameters influencing WEDM process	13
Table 3.1 Comparison of material composition Inconel 600	15
Table 3.2 Comparison of material composition Titanium grade V	16
Table 3.3 Hardness results for Inconel 600 & Titanium grade V	17
Table 3.4 Wire electrical discharge machine Specification	18
Table 3.5 Processes parameter and their levels	20
Table 3.6 Experimental plan using an L9 orthogonal array	21
Table 3.7 Experimental Conditions for WEDM	22
Table 3.8 Optical Profilometer Specifications	25
Table 3.9 Machine setting for grinding mounted samples	29
Table 3.10 Machine setting for polishing of mounted samples	30
Table 4.1 Results of kerf width	31
Table 4.2 Response table for mean kerf width	32
Table 4.3 Analysis of variance for kerf width	33
Table 4.4 Model summary for kerf width	33
Table 4.5 Optimal process parameters for kerf width	35
Table 4.6 Optimal process parameters confirmation test result for kerf width	35
Table 4.7 Results for surface roughness	36
Table 4.8 Response table for mean surface roughness	36
Table 4.9 Analysis of variance for surface roughness	37
Table 4.10 Model summary for surface roughness	38
Table 4.11 Optimal process parameters for surface roughness	40

Table 4.12 Result of confirmation test for surface roughness	40
Table 4.13 Grain distortion of WEDM samples	41
Table 5.1 Results for kerf width	43
Table 5.2 Response table for mean kerf width	44
Table 5.3 Analysis of variance for kerf width	44
Table 5.4 Model summary for kerf width	45
Table 5.5 Optimal process parameters for kerf width	47
Table 5.6 Test results for kerf width	47
Table 5.7 Results for surface roughness	48
Table 5.7 Response table for mean surface roughness	48
Table 5.8 Analysis of variance for surface roughness	48
Table 5.9 Model summary for surface roughness	49
Table 5.10 Optimal process parameters for surface roughness	49
Table 5.11 Result of confirmation test for surface roughness	51
Table 5.12 Grain distortion of WEDM samples	51

# Nomenclature

<b>WEDM</b> Wire electrical discharge Machine/machining	<b>EDS</b> Energy dispersive analysis
<b>SEM</b> Scanning electron microscopy	<b>XRD</b> Xray diffraction
<b>C</b> Peak current	<b>Pon</b> Pulse on time
<b>Poff</b> Pulse off time	<b>WFR</b> Wire feed rate
<b>DOE</b> Design of experiments	<b>Kw</b> Kerf width
<b>SR</b> Surface roughness	<b>LBM</b> Laser beam method
<b>m/min</b> Meter per minute	<b>A</b> Ampere
<b>μs</b> Micro second	<b>μm</b> Micrometers
<b>RPM</b> Revolutions per minute	<b>MRR</b> material removal rate

# CHAPTER 1

## **Introduction:**

Titanium and nickel-based alloys are suitable choices in the aerospace, automotive industry, and biomedical because these materials have high strength, low density, corrosion resistance, and high fracture. These alloys are hard to machine on traditional machining methods due to their less thermal conductivity and high reactivity. In the world of technological advancement, advanced machining processes are taking over the role of traditional methods. This phenomenon is more pronounced when it comes to cutting hard materials with complex shapes and features. Due to high heat generation, machined surfaces are liable to certain defects with few machining methods. During the cutting process, the inbuilt properties of the target material should not be varied to get desired results. Surface quality, material removal, tool cost, energy applied, and operating time should be kept in mind while the selection of appropriate machining process, otherwise it may initiate many issues which include poor surface, tool blending, work hardening, poor surface finish, other surface issues, and certainly higher production cost. Conventional machining processes often come across such issues. It is for this reason that advanced non-conventional processes machining is in high demand.

Non-conventional material processing methods such as Wire Electrical discharge machining (WEDM), Abrasive water jet machining and Laser cutting do however offer great possibilities since these methods are not sensitive to workpiece material

## **1.1 Thesis Design**

The figure shown below represents the complete analytical procedure of my research. The design shows the methodology which I have adopted during my thesis.

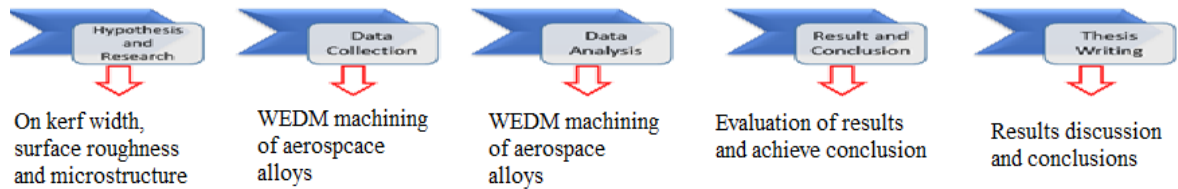


Figure 1.1 Layout for project design

## 1.2 Problem Statement

In a wire electrical discharge machine (WEDM), inappropriate choice of parameters may cause a low machining rate or poor performance. Material removal rate characteristics is the main reason behind this. Less material removal rate needs more time for the machining process and becomes extravagant and not appropriate for production. Higher material removal rates produced rough surface products and need post-processing. Therefore, a proper choice of machine parameters is required. This study goes a step further and focuses on the optimization of process parameters affecting the output parameters like kerf width and surface roughness, and their effect on grains distortion.

## 1.3 Research Objectives

Objectives of research this work are followings:

- Analyze the effect of cutting variables on kerf width
- Analyze the effect of cutting variables on surface roughness
- Finding best machine variables for kerf width and surface roughness
- Evaluation of grain distortion using SEM analysis

# CHAPTER 2

## 2.1 Literature Review:

Titanium and nickel-based alloys are the material of choice in many applications. Their high corrosion resistance, high strength and low density make them more suitable for submarine and aerospace applications. These alloys show excellent biocompatibility and can be used for prosthetic applications like orthopedic implants [1]. However, these materials are hard to process with traditional machining methods due to their less thermal conductivity and high reactivity, leading to high cutting temperature and permanent tool failure [1] [2]. WEDM is one of the advanced machining techniques which can cut conductive materials with varying hardness. Through WEDM complex geometry and intricate shapes can be cut with good dimensional precision [3]. In WEDM continuous spark is generated in the gap between the work piece and tool electrode. These successive sparks generate temperatures in the range of 8000-12000°C at the cutting edge, causing the material to melt and vaporized in that region. Material is removed in form of rubble and washed away through a dielectric fluid supply. As compared to other machining techniques WEDM required less skills and training. The choice of wire is important because of its effect on cutting speed, dimensional accuracy, and surface quality. Molybdenum wire has a high melting temperature and exceptional tensile strength and can be used in precise jobs. Moreover, molybdenum wire can be reused and thus makes the process more economical [4].

This research is conducted to find the most effective process variables controlling the surface roughness and kerf of the machined parts, and optimization of process variables that will improve the machining process. Many researchers already done a lot of work in the field of WEDM, considering different materials and parameters. Han et al.[5] Analyzed the effect of pulse duration on the single crater and material removal phenomenon behind pulse duration and current intensity. He finds out that if the pulse energy is decreased from a certain level machining process can't be performed and crater

not produce during cutting process. For higher surface finish shorter pulse duration is required. Gugulothu et al. [6] studied the effect of process parameters such as pulse on time, Poff, current and three types of dielectric fluids and their effect on the MRR and surface roughness. He finds out that drinking water as a dielectric fluid achieve maximum MRR and lower surface roughness as compared to deionized water and mixture of both drinking water and deionized water. At lower values of current the amount of material deposited is less and thus at lower current values roughness is higher. During more pulse off time dielectric fluid flush away the debris properly and thus smooth surface results with increase of pulse off time.

Okada et al.[7] Studied the dielectric fluid flow and debris motion through CFD simulation and compared it with the recorded observations of high-speed video camera. Around the wire stagnation area is observed with little flow velocity under any flow rate. The execution of debris is not fluent in that area from upper and lower nozzles, which leads to the machined kerf. Www et al. [8] analyzed the effect of peak current, WFR, Poff and Pon on material removal rate. Increasing trend of MRR is observed at higher Pon and Peak current value. When Poff decreases, then number of discharges increase in that period of time and causing high MRR.

Garg et al. [9] investigated the dimensional deviation induced by WEDM process. Six parameters were considered namely peak current, gap voltage, wire feed rate, wire tension, Pon and Poff, to analyze their effect on dimensional deviation. When Pon increases and Poff decreases then dimensional deviation increases due to increase in spark discharge energy on the work piece. Increase in voltage increase the gap between two successive sparks and thus generating less number sparks per unit time, which causes less discharge energy available in a given time. Thus, dimensional deviation decreases because of shallow craters. Shah et al.[10] Studied the effect of varying material thickness with seven machining parameters on machine output parameters, such as, MRR, kerf, and SR of tungsten carbide samples machined through WEDM. The experimental design was based on Taguchi orthogonal designs with eight controlling

parameters and three levels. It was observed that material thickness has little effect on MRR and kerf width.

S. Kumar et al. [11] uses ANFIS and GRA for optimization of machining variables such as dielectric flow rate, Pon, Poff, peak current and their influence on surface roughness and MRR. It was observed that initially at lower values of peak current SR was higher and with increase of peak current its value decreases and then after further increase in current SR value declined and becomes constant. He also finds ANFIS model provides better response. Anoop Kumar et al. [12] studied the effect of servo voltage, peak current, Pon, Poff, WFR and flushing pressure on MRR and kerf. He observed that Pon has significant effect on the SR and for kerf servo voltage is most influencing parameter.

Manikandan et al. [13] considered four nickel based super alloys and compare the SR and lower straightness and perpendicularity results of each alloy. Input parameters were Pon, Poff, WFR, current and voltage. It was observed that Monel K400 produce smaller craters because of its thermal conductivity and low melting temperature. Pon and Poff has significant on all responses. The Pon and surface roughness are in direct relation to the straightness and inversely proportional to the perpendicularity. Muralova et al. [14] considered the effect of kerf width on the machining accuracy and subsurface layer. It was observed that the kerf width dependent not only on the machine variables settings, but also depends on the mechanical and physical properties of the material being processed.

Aniah Kumar et al. [15] concluded that SR increased when Pon and  $I_p$  high values are used, this is due to large time for machining which led to the probability of double sparking and local sparking to occur. So, this double or re-sparking increases SR. Since only initial sparking is necessary to the material removal, while the following spark poorly distributed along the cutting surface and debris.

Arikatla et al. [16] Studied the effect of WFR and wire tension on MRR and width of kerf of titanium alloy. It was concluded from the experimental results that at high WFR



and wire tension the width of kerf and MRR increases. At low and high values of wire feed rate and wire tension, higher SR was observed. Intermediate values of WFR and wire tension produce smoother surface. However, it was observed that wire vibrations decreased due increase in wire tension which improves the surface finish.

## 2.2) Aerospace Alloys:

Taking advantage of greater physical and mechanical properties in relation to exceptional corrosion resistance, lasting fatigue, outstanding mechanical strength, and high strength to weight ratio of aerospace materials, therefore, in the recent past, it is preferred to use titanium and nickel alloys over structural steel material. Fig 2.1 reveals a conventional turbofan engine with main sections and the use of fundamental materials. It is quite evident that titanium and nickel-based alloys take a considerable share in the engineering of turbine discs, fan blades and pressure compressors [2].

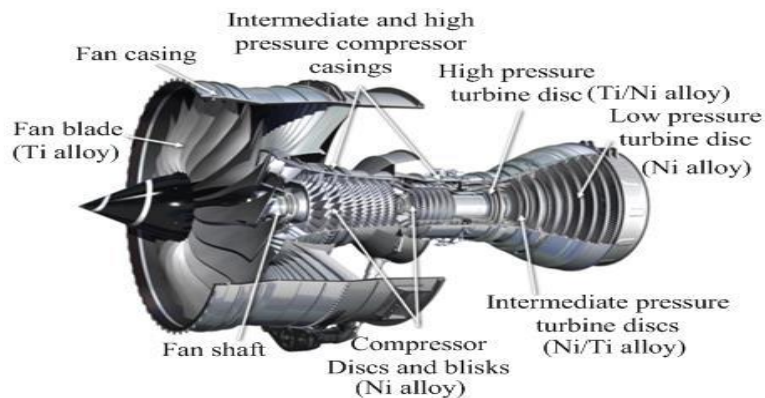


Fig 2.1 Turbofan engine of Rolls Royce showing main parts comprising titanium and nickel alloys

### 2.1.1) Titanium Alloys

#### Properties

Nickel alloys are highly corrosion and thermal resistant materials. The ability of nickel alloys which makes them a perfect material for utilizing aerospace engine's hot section

elements is that they maintain their chemical along with mechanical properties at high temperature, which can be ambient temperature up to 600° C. Statistical study/ analysis reveals that roundabout half of an aerospace engine by weight has been produced on an industrial scale by employing nickel alloys [17].

### **Conventional Cutting Problems**

Conventional machining of titanium as well as its alloys is complicated due to certain inherent properties.

- Low thermal conductivity leads to accumulation of heat which reduces life of cutting tool.
- Higher value of hardness and strength requires higher cutting forces.
- Titanium being chemical reactive at elevated temperatures with other materials causes chemical reaction between chip and tool resulting in reduced fatigue strength and tool wear.
- Lower values of elastic modulus cause poor machinability due to the chattering of work piece [17].

#### **2.1.2) Nickel Alloys**

##### **Properties**

Nickel alloys are highly corrosion and thermal resistant materials. The ability of nickel alloys which makes them a perfect material for employing in the hot section of aerospace engine components is that they maintain their chemical and mechanical properties at high temperature, which can be ambient temperature up to 600° C. Statistical study/ analysis reveals that approximately 50% weight of an aerospace engine have been manufactured by use of nickel alloys [2].

##### **Conventional Cutting Problems**

In the wake of poor machinability, nickel alloys are believed to be hard-to-cut materials that are challenging to process using traditional methods.

- The machining tool easily gets worn out and therefore, the life of the tool declines, which ultimately results in poor surface integrity.
- Since these materials can keep their higher strength combined with hardness at high cutting temperature, therefore warrants higher values of cutting forces.
- Lower value of thermal conductivity of these alloys results in heat accumulation at tool/ target material during the machining process. As a result of thermos-mechanical stresses brought in by cutting temperature gradients and high cutting force, alterations in microstructure and mechanical properties is obvious besides machined surface damage.

Even some non-traditional techniques such as laser machining (LM) and Abrasive water jet machining (WAJM) are also not an effective method due to heat affected zone and taper effect [2].

## **2.2) Wire Electrical Discharge Machining**

### **2.2.1) Introduction**

Joseph Priestley an English Physicist in 1770, investigated the electrical discharges erosive outcomes. Advancing the Priestley's research, the EDM process was developed by two Russian scientists. They invented a stabilized system for machining of metals. In 1952, first machine was designed, on the principle of spark erosion by a manufacturer Charmilles and was available for the first time at the European Machine Tool Exhibition. Recently, the machine speed has increases up to 20 times, this leads to decrease in processing cost and improved the surface quality.

Wire electrical discharge machine technology comes as an emerging new technology that could handle the cutting of almost all types of materials and profiles in a non-conventional way. After milling, turning and grinding WEDM is the fourth most popular machining method.

### **2.2.2) Working Principle**

Wire electrical discharge machine works on the principle of spark erosion, sometimes referred as Spark machining. Material is eroded from the workpiece by continuously reoccurring sparks between two electrodes, immersed in a dielectric fluid and subject to

an electric voltage. Schematic diagram given below explains the basic working of wire electrical discharge machining.

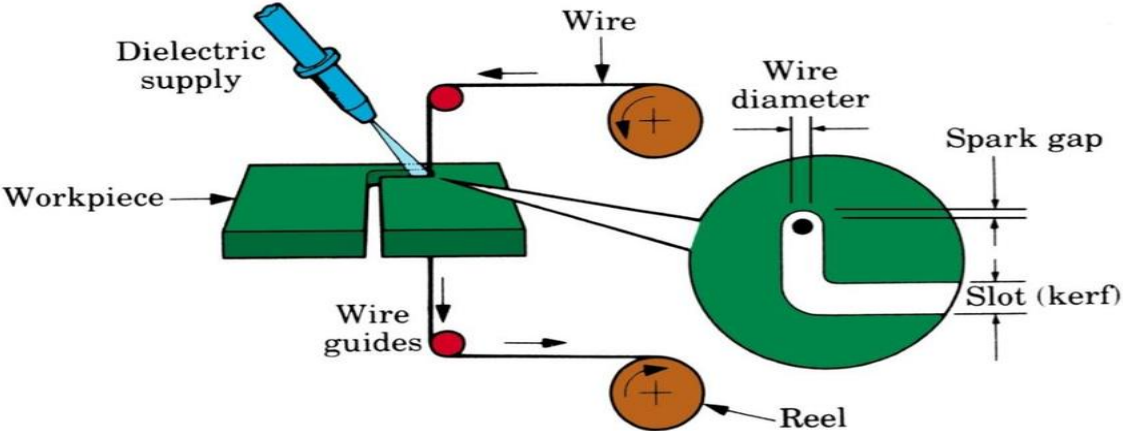


Figure 2.2 Working principle of wire electrical discharge machine

**2.2.3) Main Components and Working**

A typical schematic sketch of EDM machine is shown in Fig. 2.3

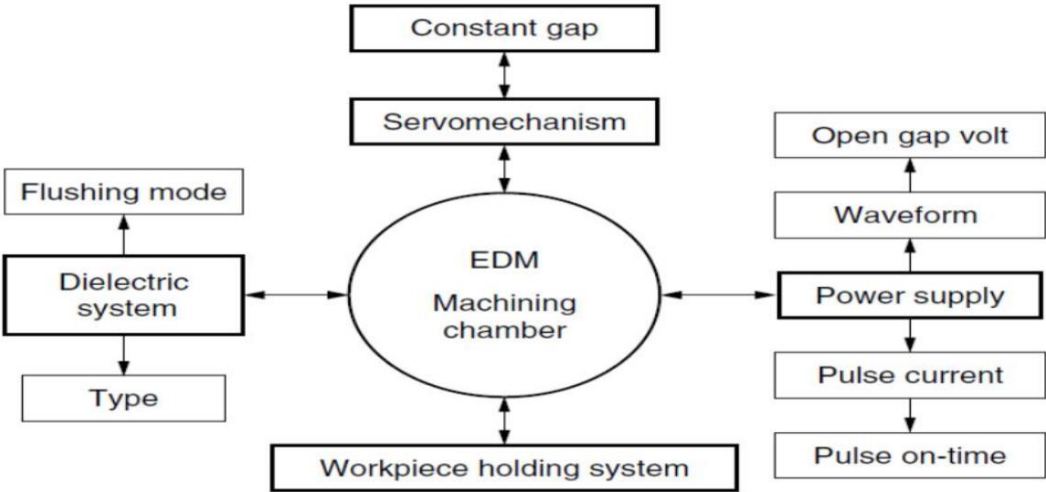


Figure 2.3 Components of WEDM Machine

Major components of WEDM are machine body, coordinate worktable, filament system, wire rack, work liquid circulation system and electrical and numerical control system. The coordinate worktable is controlled by numerical control system, enabling the work

piece to make precise traverse and longitudinal movement as per given track, and enabling the filament make back and forth straight movement at high speed.

### **Machine Body**

The body is a case type cast iron piece, incorporating electrical and work liquid cases on two sides or internally and worktable, filament system, lightning and other systems on top.

### **Electric power supply**

Both the work piece and tool electrodes are electrically linked to a direct current power supply.

### **Coordinate worktable**

The worktable mainly constituted of table pulling plate, middle pulling plate, precise screw pair and gearbox. The vertical and horizontal movement of pulling plate is of rolling guide rail structure.

### **Filament movement**

The filament moving device realizes the straight reciprocating motion of electrode filament and its circulation application. The filament storage is constituted of hollow cylinder which is isolated from the principal axis. The filament motion motor is connected with the filament storage reel by coupling.

### **Filament rack**

The filament rack is constituted of column, fixed arm, sliding arm and guide wheels with good rigidity. The front part of filament rack is equipped with hard alloy power input block, guide wheel with power input isolated from filament rack arm. The electrode filament goes from wire filament storage reel to the principal guide wheel in the head of filament rack through up and low spraying nozzles. There is a water valve in the bottom of column with two taps to regulate the work liquid volume of up and low spraying nozzles in the filament arm through the valve.

### **Work liquid tank**

A dielectric counteracts an electric field, and suppresses electrical discharges. Normally kerosene oil or deionized water is used as a dielectric. The gap between tool and work piece is insulated by dielectric fluid, cool down the tool and work piece and flushes the metal particle. A pump sends work liquid to spraying nozzles. This liquid returns to the tank through the receiving grooves in the worktable and recirculated after passing through the filter.

### **Auxiliary part**

Fixture, handles and lighteners are used for assistance during processing.

### **Work piece and tool**

Usually, work piece act as an anode and tool electrode as cathode.

#### **2.2.4) Wire Used**

Molybdenum wire of dia 0.18mm was used as a cutting tool. Molybdenum wire has high melting point and tensile strength. Moreover, molybdenum wire can be reused and makes the process more economical as compare to other wires like steel, brass and copper wire. Dimensional accuracy increases as the wire tension increases, because wire vibrates during cutting process. With molybdenum wire more tension can be applied because of its high tensile strength. This wire reduces the chances of wire breakage due to its high melting point and resistance to thermal loads [4].

#### **2.2.5) Advantages of WEDM**

WEDM is an emerging cutting technology, which has many plus points over the other non-conventional cutting techniques.

- Can machine any conductive material with varying hardness
- Process is highly accurate and can achieve good surface finish results
- Non-contact process and involves no cutting forced
- Complex geometries can be machined at average tool cost

- Holes can be completed in one pass

### **2.2.6) Applications of Wire electro Discharge Machining**

WEDM is useful in many areas of modern industry, such as aerospace industry, automotive industry, chemical process engineering, and construction engineering and environmental technology.

### **2.2.7) Limitations of Wire Electro Discharge Machining**

- Can process conductive materials only
- For high quality surface finish products overall process will be slow
- Vapors of dielectric fluid in high energy density applications are harmful
- Small heat affected zone near cutting edges

### **2.2.8) WEDM process parameters**

The material removal procedure because of contact between the target material and WEDM is firmly governed by several parameters which can be categorized as parameters of input and output. The course of action of WEDM is dealt by many process parameters shown in Table 2.1, which qualify the cost of budget, efficacy, and quality of the complete process.

Table 2.1 Process variables affecting WEDM process

Input Parameters	Output Parameters
Peak current	Surface roughness
Pulse width	Kerf width, top and bottom
Pulse duration	Depth of cut
WFR	MRR
Wire tension	Tool wear rate
Flushing pressure	Striation formation
Spark gap, wire material and diameter	

### 2.3) Flow Chart for Experimentation

Following sequence is followed for experimentation work as shown in the figure 2.4 given below

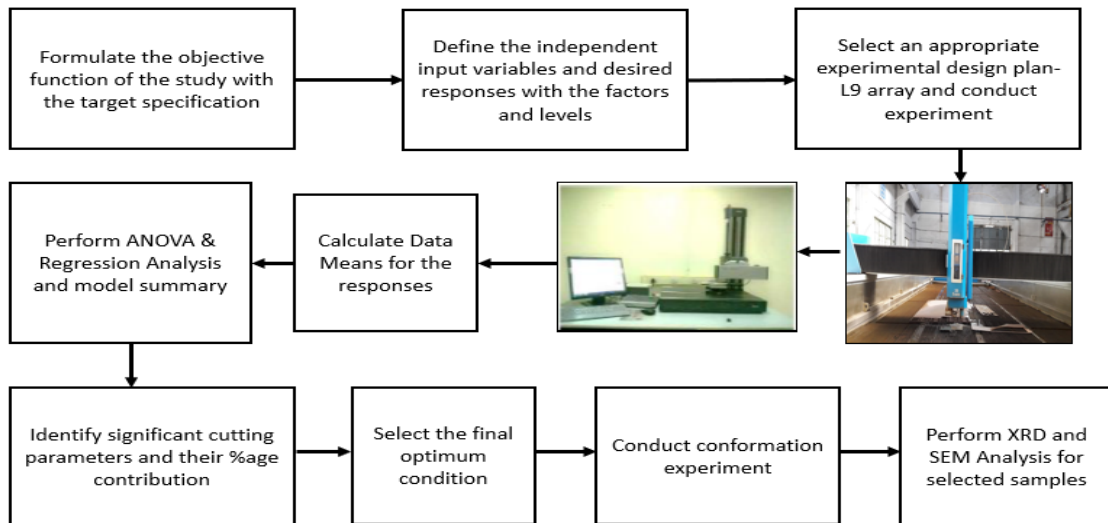


Figure 2.4 Flow chart for experimentation



# CHAPTER 3

## EXPERIMENTATION AND CHARACTERIZATION TECHNIQUES

### 3.1) List of Equipment

There is different type of equipment's used for the experimentation. These equipment's can be categorized into the machining equipment, data collection equipment and analysis equipment. The details and specification of the equipment will be discussed later in the experimentation section. The list of equipment that are used for the experimentation are given bellow.

1. Wire Electrical Discharge Machining
2. Metallurgical microscope MT-8530
3. Optical Profilometer
4. Scanning electron microscope (SEM)
5. XRD machine

### 3.2) Work Piece Material

Inconel 600 and Titanium grade V are used in the experimentation for this research work. The samples are cut into the shape of circular bar using machine. The measurement of the work piece material is 18mm $\phi$  and 4mm thickness.

### 3.3) EDS Analysis

Composition test was done on both samples using scanning election microscope to find the exact specification of the material. Three tests were conducted on different spots.

### 3.3.1) Inconel 600

The result of the EDS analysis for Inconel600 is given in Table 3.1. SEM image taken while composition test and EDS spectrum is shown in Figure 3.1

Table 3.1 Comparison of material composition Inconel 600

Element	Nickel	Chromium	Iron	Carbon	Manganese	Cobalt	Total
% Weight	72.42	15.76	6.67	4.54	0.41	0.21	100

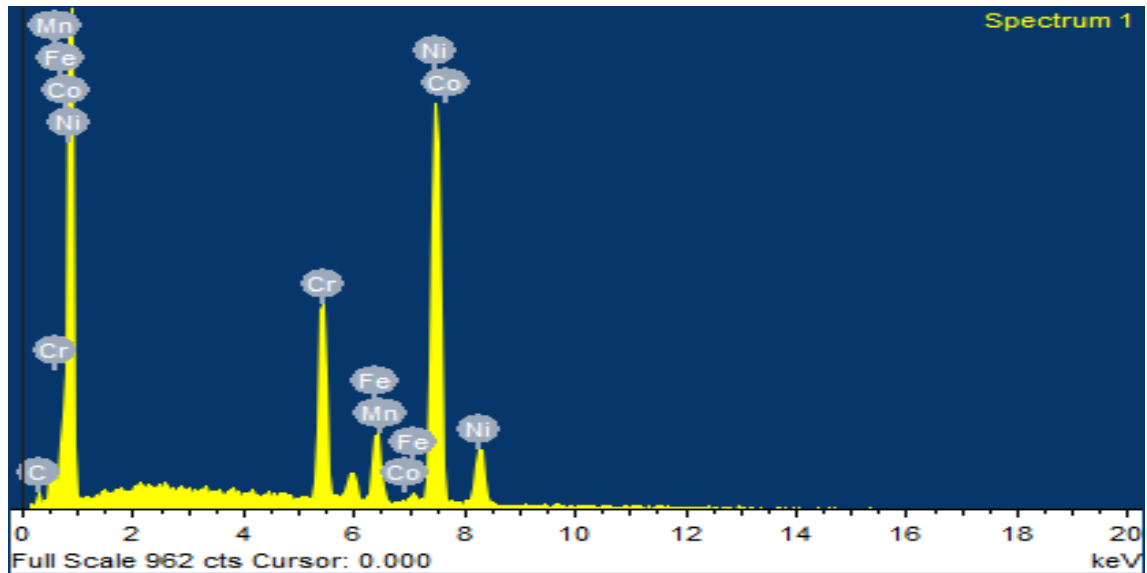


Figure 3.1 EDS spectrum of Inconel 600

### 3.3.2) Titanium Grade V

The result of the EDS analysis for Titanium grade V is given in Table 3.2 EDS spectrum and SEM image taken while composition test is shown in Figure 3.2

Table 3.2 Comparison of material composition Titanium grade V

Element	Titanium	Aluminum	Vanadium	Molybdenum	Palladium	Total
% Weight	90.02		2.06	0.50	0.32	100

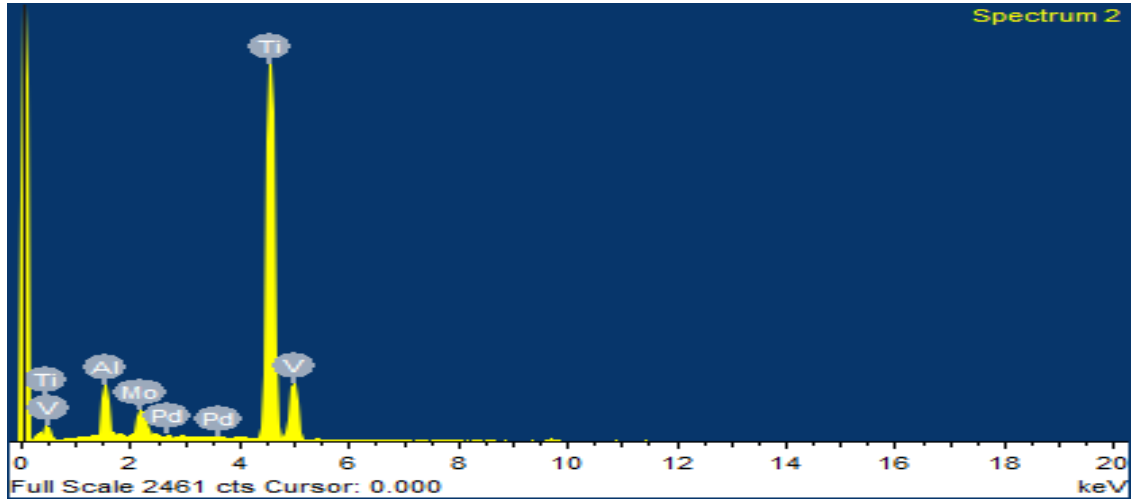


Figure 3.2 EDS spectrum of titanium grade V

### 3.4) Mechanical Properties

#### 3.4.1) Vickers Hardness Test

Micro hardness tester is used to find the hardness of Inconel 600 and Titanium grade V. Five tests were conducted on different areas to be more accurate. Dwell time was 15sec and 1 Kgf force was used during these tests.

#### 3.4.2) Rockwell Hardness Test

To find the Rockwell hardness of Inconel 600, 10 Kgf steel ball and for Titanium grade V diamond ball 10 Kgf. Is used. Five tests were conducted on different areas to be more accurate.

### 3.4.3) Test Results

Vickers hardness and Rockwell hardness test results for both materials are shown in the table given below

Table 3.3 Hardness results for Inconel 600 & Titanium grade V

Material	Vickers Hardness No	Rockwell Hardness No
Inconel 600	192	81 to 82 HRC
Titanium Grade V	340 to 342	30 HRC

### 3.5) Wire Electro Discharge Machine

Wire electro-discharge Machine installed at MRC NUST is used to cut samples by using different parameters for the experimentation. The specifications for the wire electro-discharge machine are given in Table 3.4



Figure 3.3 Wire Electro Discharge Machine

Table 3.4 Wire Electro-discharge machine specification

S No	Parameter	Specification
1	Model	DK 7732AZ
2	Cutting Thickness	300mm
3	Table Travel	320x400mm
4	Peak Current	0.5-10A
5	Max. Cutting Speed	150 mm <sup>2</sup> /min
6	Pulse Width	2-128 $\mu$ s
7	Pulse Interval	5-15 $\mu$ s
8	Voltage	70-120 V
9	Wire D $\phi$	0.18mm $\phi$

### 3.6) Wire Used

Molybdenum wire of 0.18mm $\phi$  is used for cutting samples.

### 3.7) Selection of Process Parameters

Surface roughness, kerf width, material removal rate, and depth of cut have all been considered responses, but researchers have discovered that peak current, pulse width, pulse interval, and wire feed rate and voltage as influential variables in WEDM process. Following criteria is used for the selection of different level of parameters.

#### 1) Peak Current (A)

It is the power utilized in electrical discharge machining and measured in amperages. During the pulse on time, the current reaches to a preset level, which is called as the peak current. In WEDM process, peak current means maximum amperages utilized by

the surface area of the cut. Higher values of peak currents are used to increase MRR, thus produce rough surface finish products.

## **2) Pulse on time ( $\mu\text{s}$ )**

The pulse on time is denoted as  $P_{on}$  and it shows the time duration in micro seconds ( $\mu\text{s}$ ) in which discharge energy is applied in the gap between tool electrode and workpiece. Higher discharge energy is applied when high pulse on time value is used.

## **3) Pulse off time ( $\mu\text{s}$ )**

The pulse off time is denoted as  $P_{off}$ . It is the time duration between the two successive sparks and it is measured in micro seconds. This is actually the time between successive sparks. During Pulse off time there is no effect on the discharge energy. During pulse off time discharges are paused and debris solidify and flushed away by dielectric fluid before next discharge. At lower values of pulse off time large number of discharges are produced in a given time, which increase sparks energy as a result cutting rate increased. However lower of pulse off time can affect the tool life.

## **4) Wire feed rate (m/min)**

It is the rate at which wire electrode travels along the guided path for continuous sparking. In WEDM wire electrodes can save 70% of material processing cost. So, for longer tool life lower WFR are desirable.

### **3.8) Taguchi Methodology and Design of experiments**

Design of experiment (DOE) was first established by R.A Fisher. This is a statistical technique that is employed to check the response of several parameters simultaneously. Dr Taguchi basically was a researcher in electronics lab that further pursue research on design of experiments. He spent a lot of time to make this technique very effective and easy to use. DOE is very productive technique to enhance the qualities of manufacturing activities. This method provides a simple, systematic and approach for an optimal design to excess the performance, cost and quality. This design of experiments was used to

minimize the number of experiments in order to reduce cost and time. Four cutting parameters and the level of machining parameters are given in table 3.5

Table 3.5 Processes parameter and their levels

<b>Parameter</b>	<b>Units</b>	<b>Level 1</b>	<b>Level 2</b>	<b>Level 3</b>
Peak Current(C)	A	1	2	3
Pulse on time(Pon)	μs	32	64	128
Pulse off time(Poff)	μs	5	7	9
Wire feed rate(WFR)	m/min	20	30	40

Based on process parameters and their levels a Taguchi L9 orthogonal array is used to define 9 trials by using MINITAB 19 software. Each of the 9 trial and their parameters are given in table 3.6

Taguchi      L9(3<sup>4</sup>)

Array

Factors:      4

Runs:         9

Table 3. 6 Experimental Plan using an L9 orthogonal array

S No	C	Poff	Pon	WFR
1	1	5	32	20
2	1	7	64	30
3	1	9	128	40
4	2	5	64	40
5	2	7	128	20
6	2	9	32	30
7	3	5	128	30
8	3	7	32	40
9	3	9	64	20

### 3.9) Methodology

The experiments were done on Inconel 600 and Titanium grade V. The experiments were performed on Wire electrical discharge machine, cutting thickness of the work piece was 4mm. Molybdenum wire was used as tool electrode because of its high tensile strength and load carrying capacity. Total 72 samples were cut for both alloys by cutting four samples against each combination from experimental plan (L9 Array) obtained from DOE for each material. Experimental settings for these tests are given in table 3.7



Table 3.7 Experimental settings for WEDM

<b>Workpiece</b>	Inconel 600 & Titanium Grade V
<b>Voltage</b>	100 v
<b>Stand of distance</b>	0.065 mm
<b>Workpiece dimension</b>	Diameter: 18mm, Thickness: 4mm
<b>Wire</b>	Molybdenum wire of dia 0.18mm
<b>Dielectric fluid</b>	Water soluble cutting oil

For kerf width analysis a horizontal center cut of 9 mm was made on 36 samples for both alloys as shown in figure 3.4

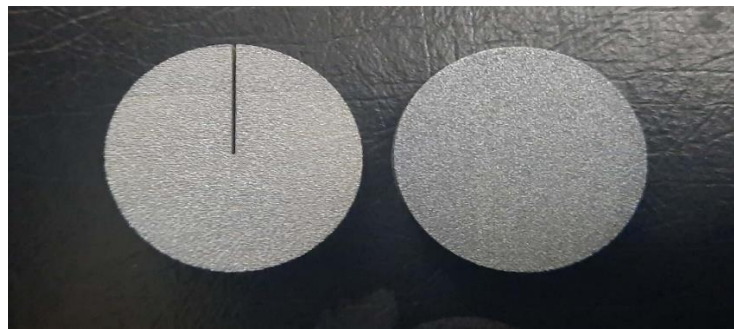


Figure 3.4 Samples after WEDM

### 3.10) Measurement of Response Parameters

Following response parameters were selected.

#### 3.10.1) Kerf Width ( $\mu\text{m}$ )

The geometry of kerf is an attribute of key concern in WEDM as it generally opens a slot which is slightly tapered in precision jobs. The top width ( $W_t$ ) is broader than the width of the bottom ( $W_b$ ) as shown in Figure 3.7. The perpendicularity or straightness of the cut gets worse by the larger kerf width which results in inaccurate dimensional quality.

$$\text{Kerf width: } \frac{(wt + wb)}{2}$$
 \_\_\_\_\_ Equation (1)

$Wt$  = Top Kerf width  
 $Wb$  = Bottom Kerf Width

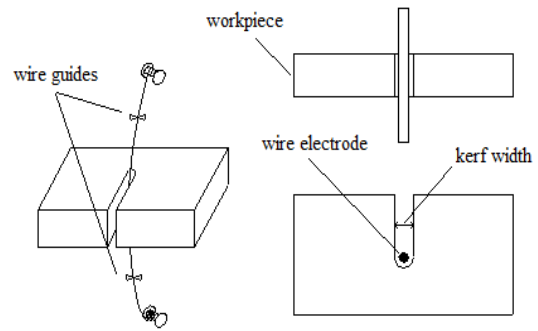


Figure 3.5 WEDM CUT and kerf

The measurement of width of top kerf ( $Wt$ ) and width of bottom kerf ( $Wb$ ) was done with the help of Metallurgical microscope using lens 5X and kerf width was computed with the help of equation 1. Metallurgical microscope use for for measurements is shown in figure 3.6



Figure 3.6 Metallurgical Microscope

Two values for kerf width were recorded per specimen and their mean value was used for kerf analysis. Images recorded from optical microscope for sample of Inconel 600 are shown in Figure 3.7 (a) & ;(b).

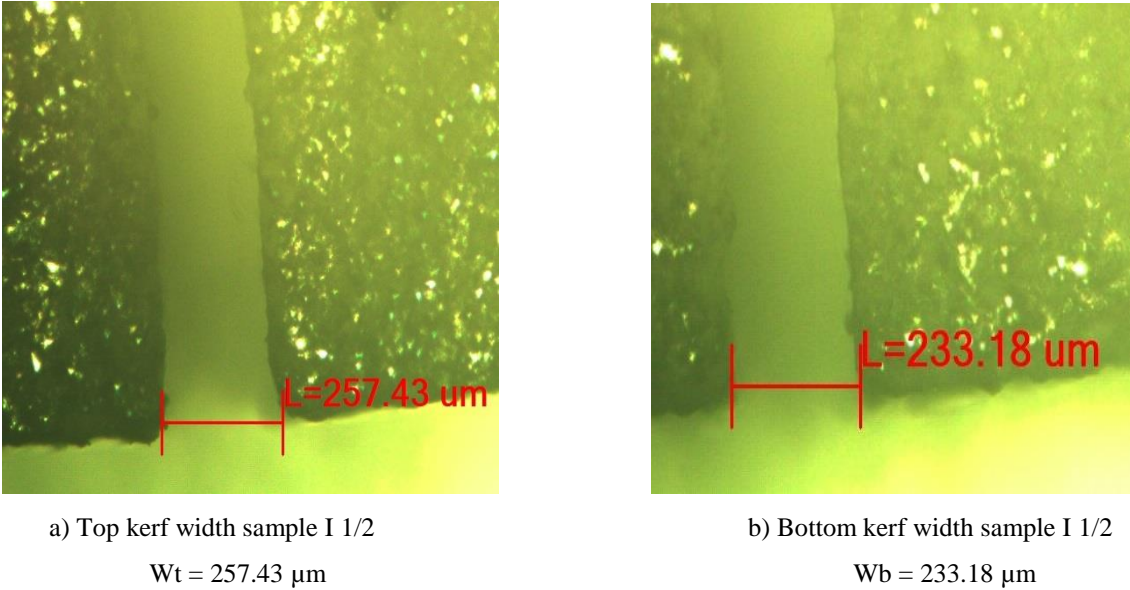


Figure 3.7 a & b Images from optical microscope

**3.10.2) Surface Roughness (μm)**

The measure of finely spaced surface irregularities is called surface roughness. Surface roughness performs a vital part in obtaining dimensional accuracy therefore, choice of process parameters is of utmost importance for acquiring superior surface finish. Surface roughness was measured using an Optical profilometer PS Nanovea 50. Two readings were recorded against each set of L9 array and mean value was considered for analysis. Surface roughness values were measured in micrometers. Figure 3.8 shows optical profilometer used for surface roughness measurements and its specification are given in table 3.8

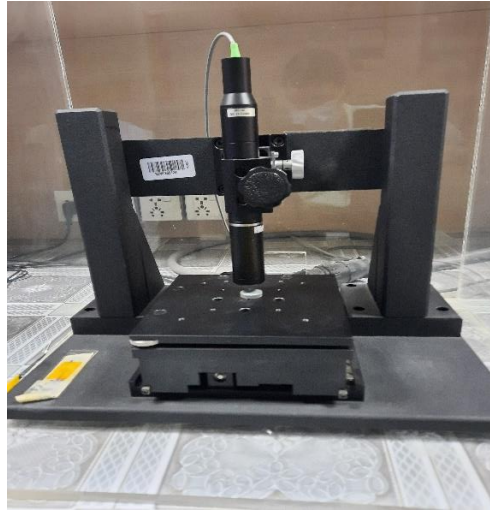


Figure 3.8 Optical Profilometer

Table 3.8 Optical Profilometer Specifications

<b>Optical Profilometer Specifications</b>	
Company	Nanovea
Model	PS 50
Test Facility	Thickness and topography of thin films
X-Y Axis Travel	50 mm
X-Y Axis Resolution	0.1 $\mu\text{m}$
Vertical Resolution	12 nm

Surface roughness profile of a sample is shown in Figure 3.8 with surface roughness value of  $4.62\mu\text{m}$  and scan length of 12mm.

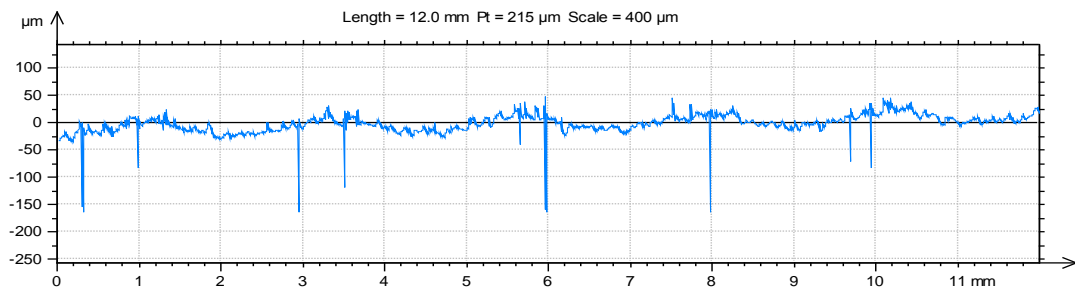


Figure 3.9 Surface roughness profile of Sample T-6/2

### **3.11 Analysis of variance (ANOVA)**

Variance analysis is a statistical tool that is used to explain the experimental results and also employed to check the variation in average performance of groups of items tested. The purpose of variance is to check the variation of individual factor relative to the total variation observed in the result. ANOVA was achieved with the aid of MINITAB 19 software to investigate the outcome of parameters of machining on kerf angle and surface roughness with the help of percentage contribution. For a 95% confidence level ( $\alpha = 0.05$ ), a detailed analysis was carried out. Based on these results the significance of machining parameters on kerf width and surface roughness was calculated. In ANOVA analysis the value of P and F play a key role to decide the significance of factors. If the value of P is less than 0.05 then the factor is considered as significant. Moreover, the larger F-value showed the importance of input factor. Based on these results the significance of machining parameters such as peak current, wire feed rate, pulse on time and pulse off time on kerf width and surface roughness was calculated.

#### **3.11.1) Regression Analysis**

Regression analysis is used to evaluate regression coefficients that minimize the error and also predictions from the developed regression models were compared with measured kerf width and surface roughness. Regression equations were obtained for surface roughness and kerf width. This mathematical model provides a good relationship between machining parameters and output parameters. Capability of the model was tested with the help of coefficient of determination  $R^2$ .

#### **3.11.2) Confirmation of test**

It is the final step in DOE process. Experimental confirmation test was carried out for kerf width and surface roughness for both alloys, to verify the results based on experimental design.

### 3.12) SEM Analysis

#### 3.12.1) Sample Preparation

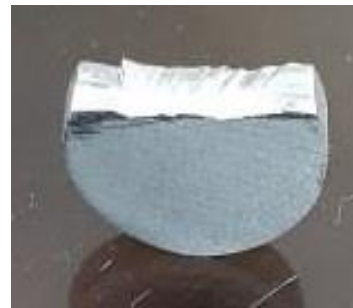
The following steps were adopted for the sample preparation before conducting SEM analysis.

#### 3.12.2) Sample Cutting

To study the microstructural changes along the border of the sample and to get a small flat surface to facilitate the mounting process a small section of sample was cut using hand saw.



(a) Sample after WEDM



(b) Sample after hand saw cut

Figure 3.10 Machined sample before mounting

#### 3.12.3) Sample Mounting

For analyzing the microstructure, first we need to make a mold in which sample was placed. For making the mold, mounting mechanism is the most appropriate method. Sample was placed on the vertical placement bar of “Hydro- press mounting Machine “which is also called Automatic Mounting Machine. Shower the specific amount of Conductive mount Bakelite powder over the sample and covered the mounting press with a plunger. Set the temperature T (Su) of 180 o C and pressure 270 bar, wait for 20 minutes to achieve the mounted sample. After completion of cycle, machine beep would be heard, which is basically the indication to collect your sample. This process was used for all selected

samples. Hot mount Hydro-press mount machine used for mounting of samples is shown in figure 3.11 and mounted sample is shown in figure 3.12.



Figure 3.11 Hydro-press mounting machine

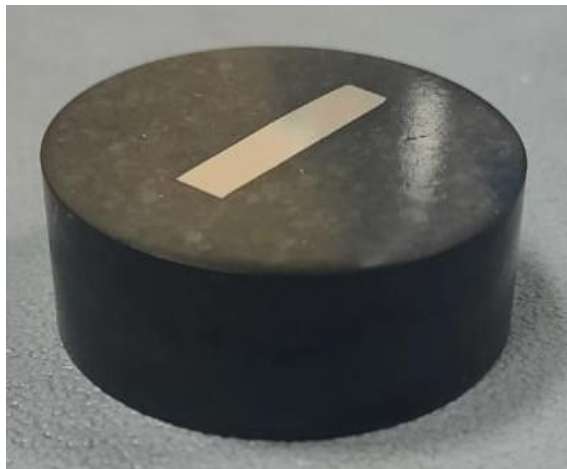


Figure 3.12 Mounted Sample

#### 3.12.4) Sample Grinding

Mounted samples were then grinded by using different abrasive grinding papers, i.e. Silicon Carbide (waterproof) grinding papers with the help of automatic grinding and polishing machine. The various parameters for machine setting are given in Table 3.9.



First, the mounted samples were grinded by using 320 and 800 silicon carbide grinding papers to trim mold surface. Then shifted to 1200, 2000 and 2400 at the end when the surface was nearly finished (smooth), 4000 abrasive grinding paper was used. When shifting the mounted sample from one silicon carbide grinding paper to another it was washed with water and ethanol. Figure 3.13 represents automatic grinding and polishing machine.



Figure 3.13 automatic grinding and Polishing Machine

Table 3.9 Machine setting for grinding mounted samples

Grinding Force	Time	RPM Head	RPM Bed
3 DaN	3 min onwards	250	150

### 3.12.5) Sample Polishing

Polishing of the mounted samples was done using automatic grinding and polishing machine. Extra fine and smooth surface was the main objective. Polishing pads from 3  $\mu\text{m}$  to 0.05  $\mu\text{m}$  were used along with their respective colloidal suspensions. When shifting the mounted sample from one polishing paper to another it was washed with water and ethanol and surface was observed using optical microscope at each stage.



Various machine parameter settings along with the time taken for polishing against each polishing pad is given in Table 3.10.

Table 3.10 Machine setting for polishing of mounted samples

Polishing Pads	Grinding Force	Time	RPM Head	RPM Bed
3 $\mu\text{m}$	1.5 DaN	10 min	150	100
1 $\mu\text{m}$	1.5 DaN	10 min	150	100
0.5 $\mu\text{m}$	1.5 DaN	20 min	150	100
0.05 $\mu\text{m}$	1.5 DaN	300 min	150	100

Scanning electron microscopy was used for selected samples of both alloys to measure the grain distortion after WEDM using ImageJ software.

### 3.13) XRD Analysis

Diffraction of X-rays from crystal structure is a strong technique to determine lattice planes, stress, strain, and phases. X-rays are high energy waves, which when collide to a material, are scattered according to the atomic locations in the crystal. This is due to periodic arrangement of atoms. Scattered rays which are out of phase show destructive interference. The XRD analysis was done using Xpert PRO PAN Analytical machine to check the phase changes in machined samples. The wavelength used was 1.54 Angstrom and source was Copper tube. Jad65 software was used to plot the peaks data.

# CHAPTER 4

## Wire Electro Discharge Machining of Inconel 600

### Results and discussion

Present work is designed to predict the surface roughness and Kerf width of Inconel 600 and analyze the effect of WEDM parameters on surface roughness and kerf width. ANOVA is used to obtain the most significant factors for each response variable.

#### 4.1) Kerf width results

Kerf width of each machined sample is measured through metallurgical microscope using 5x lens are discussed in chapter 3. The obtained results from experimental data are given in table 4.1

Table 4.1 Results of kerf width

S No	C	Poff	Pon	WFR	Kw
	Ampere	$\mu\text{s}$	$\mu\text{s}$	m/minute	$\mu\text{m}$
1	1	5	32	20	0.27982
2	1	7	64	30	0.27329
3	1	9	128	40	0.32179
4	2	5	64	40	0.34418
5	2	7	128	20	0.32086
6	2	9	32	30	0.28899
7	3	5	128	30	0.36015
8	3	7	32	40	0.31107
9	3	9	64	20	0.29230

#### 4.1.1) Response Table for Data Means

ANOVA is performed on data means of kerf width and ranking of each input parameter is given in table 4.2

Table 4.2 Response table for mean kerf width

<b>Level</b>	<b>C</b>	<b>Poff</b>	<b>Pon</b>	<b>WFR</b>
1	0.2916	0.3281	0.2933	0.2977
2	0.3180	0.3017	0.3033	0.3075
3	0.3212	0.3010	0.3343	0.3257
Delta	0.0295	0.0270	0.0410	0.0280
Rank	2	4	1	3

#### 4.1.2) Analysis of Variance

Using ANOVA percentage contribution of each variable is calculated and F and P values obtained from ANOVA table decides the significance of a factor. A factor will be considered as significant if its F-value is higher and P-value should be less than 0.05. The results shows the pulse on time significance for kerf width with percentage contribution of 39.40% and P-value is 0.015. Table 4.3 shows percentage contribution and significance results of the parameters.

Table 4.3 Variance analysis for kerf width

Source	DF	Adj SS	Adj MS	Contribution	F-Value	P-Value	Significance
Regression	4	0.006295	0.001574		9.56	0.025	
C	1	0.001309	0.001309	22.69%	7.95	0.048	Significant
Poff	1	0.001095	0.001095	20.46 %	6.65	0.061	Not significant
Pon	1	0.002713	0.002713	39.40 %	16.48	0.015	Significant
WFR	1	0.001178	0.001178	17.44%	7.15	0.056	Not significant
Error	4	0.000659	0.000165				
Total	8	0.006954					

#### 4.1.3) Regression Equation

Regression equation obtained from analysis of variance results is given below

$$\text{Kerf Width} = 0.2535 + 0.01477 C - 0.00676 \text{ Poff} + 0.000435 \text{ Pon} + 0.001401 \text{ WFR}$$

#### 4.1.4) Model Summary

The values of R<sup>2</sup> and R<sup>2</sup> adjusted are between 81 to 90 % as shown in Table 4.4. This Shows that regression model provides a good relationship between process and response Parameters. This means that 81.06 % variability of system is explained by the considered model.

Table 4.4 Model summary for kerf width

S	R-sq	R-sq(adj)	R-sq(pred)
0.0128308	90.53%	81.06%	68.32%

#### 4.1.6) Data Means Plot

In data means plot four factors (Peak current, pulse off time, pulse on time, wire feed rate) are used as input and response variable was kerf width. The data means plot analysis basically used to check to check the effects of individual factor on response variable. Figure 4.1 shows the plot of input parameters and response variable.

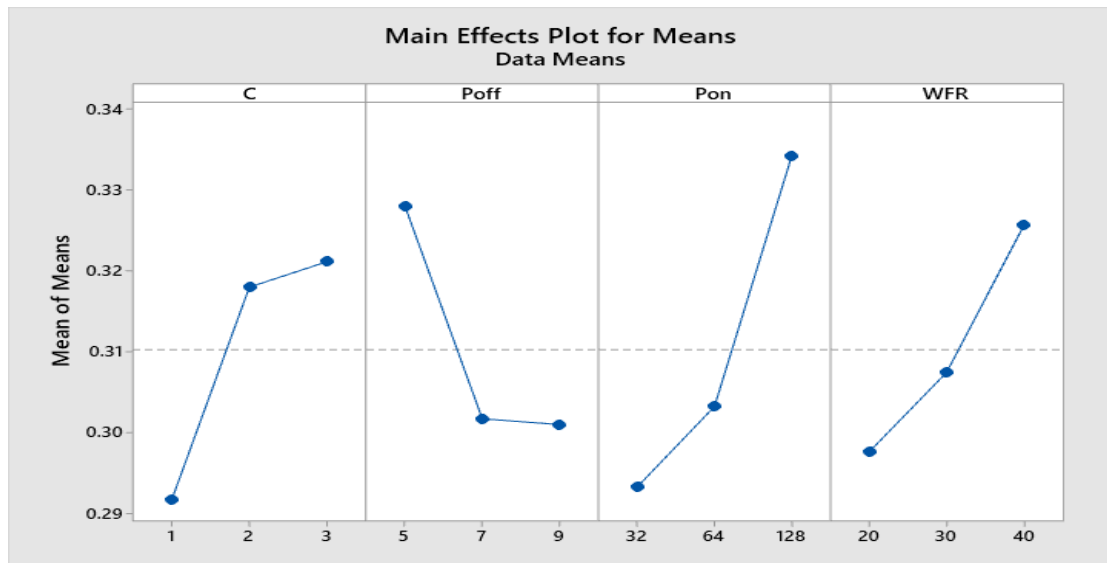


Figure 4.1 Main effect plots of data means for kerf width

## 4.2) Kerf Width Analysis

The data effect plot for means in figure 4.1 shows the variation of kerf width with respect to selected process parameters. The effect of each individual parameter on kerf width is discussed below.

### 4.2.1) Peak Current (C)

Kerf width increases with increase in peak current value and it is the second most influencing parameter on kerf width. This increasing trend is because with increase in

peak current wire displacement and vibration in wire increases which results in bigger kerf width

#### **4.2.2) Pulse of time (Poff)**

Pulse off time has very negligible effect on kerf width and its percentage contribution is very low and almost negligible.

#### **4.2.3) Pulse on time (Pon)**

Most influencing parameter for kerf width observed in this study for Inconel 600 is pulse on time. Kerf width increases with increase in pulse on time, this is because more discharge energy is available for longer period of time. Pon is the most significant factor with the percentage contribution of 39.40% obtained from ANOVA results [18].

#### **4.2.4) Wire Feed Rate (WFR)**

Kerf width increases with increase in wire feed rate but the effect is very little, which can be seen from the plot.

### **4.3) Optimal Process Parameters**

Optimal set of parameters is obtained from the data means plot and given in table 4.5

Table 4.5 Optimal process parameters for kerf width

Process Parameter	C (A)	Poff ( $\mu$ s)	Pon ( $\mu$ s)	WFR (m/min)
Optimal Setting	1	9	32	20

#### **4.3.1) Confirmation Test**

Confirmatory test is conducted to verify whether the optimal value of factors will achieve low kerf width. The model considered is adequate as results obtained from confirmatory test are satisfactory.

Table 4.6 Optimal process parameters confirmation test result for kerf width

Response	Predicted Mean	Actual value	% Error
Kerf Width	0.252797	0.25348	0.26%

#### 4.4) Surface Roughness Results

Surface roughness of each sample is calculated using optical profilometer. Each sample is scanned up to 12mm length. The results are given in the table 4.7

Table 4.7 Results for surface roughness

S No	C	Poff	Pon	WFR	SR Mean (Ra)
	Ampere	$\mu\text{s}$	$\mu\text{s}$	m/minute	$\mu\text{m}$
1	1	5	32	20	7.91
2	1	7	64	30	6.85
3	1	9	128	40	6.32
4	2	5	64	40	5.98
5	2	7	128	20	6.65
6	2	9	32	30	5.21
7	3	5	128	30	6.87
8	3	7	32	40	5.03
9	3	9	64	20	6.80

##### 4.4.1) Response Table for Data Means

ANOVA results for surface roughness data means smaller is better approach given in table 4.8 showing the ranking of each input parameter.

Table 4.8 Response table for mean surface roughness

Level	C	Poff	Pon	WFR
1	-16.90	-16.75	-15.44	-17.02
2	-15.44	-15.73	-16.30	-15.93
3	-15.81	-15.67	-16.40	-15.19
Delta	1.45	1.08	0.96	1.83
Rank	2	3	4	1

#### 4.4.2) Analysis of Variance

Through analysis of variance input variables percentage contribution is calculated, from their F and P-value significance of a parameter is obtained. From table 4.9 it is observed that WFR is the most significant factor for surface roughness with percentage contribution of 42.88% and p-value 0.049.

Table 4.9 Variance analysis for surface roughness

Source	DF	Adj SS	Adj MS	Contribution	F-Value	P-Value	Significance
Regression	4	5.0206	1.2551		3.64	0.120	
C	1	0.9441	0.9441	29.33%	2.73	0.174	Not Significant
Poff	1	0.9842	0.9842	18.94 %	2.85	0.167	Not significant
Pon	1	0.3856	0.3856	8.83%	1.12	0.350	Not Significant
WFR	1	2.7068	2.7068	42.88%	7.84	0.049	Significant
Error	4	1.3812	0.3453				
Total	8	6.4018					



**4.4.3) Regression Equation**

Regression equation obtained from analysis of variance results is given below  
Surface Roughness= 10.24 - 0.397 C - 0.203 Poff + 0.00519 Pon - 0.0672 WFR

**4.4.4) Model summary**

Model summary was tested at 95% confidence level and R-sq(adj) value is 56.85% which means that 56.85% variability of the data is explained by the model Considered. Model summary results are shown in table 4.10

Table 4.10 Model summary for surface roughness

<b>S</b>	<b>R-sq</b>	<b>R-sq(adj)</b>	<b>R-sq(pred)</b>
0.587614	78.43%	56.85%	0.00%

**4.4.6) Data Means Plot**

In data means plot four factors (Peak current, pulse off time, pulse on time, wire feed rate) are used as input and response variable was surface roughness. The data means plot analysis basically used to check the effects of individual factor on response variable. Figure 4.3 shows the plot of input parameters and response variable.

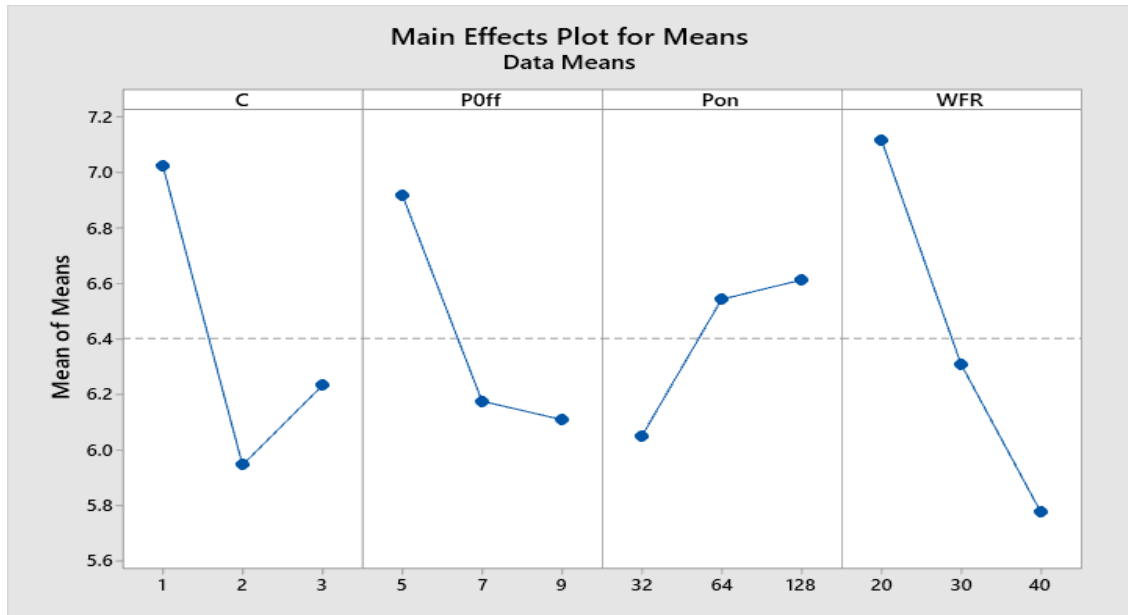


Figure 4.2 Main effect plot for data means for surface roughness

## 4.5) Surface Roughness Analysis

The data effect plot for means in Figure no 4.2 shows the variation of surface roughness with respect to other selected process parameters explained as under,

### 4.5.1) Peak Current (C)

At initial value of peak current surface roughness increases and then decreases at intermediate values of current with further increase in current the surface roughness increases. When peak current increases then surface roughness increases because of larger crater formation. Peak current was observed second most significant factor with percentage contribution of 29.33%. Medium peak current levels are required for better surface finish[18].

### 4.5.2) Pulse off time (Poff)

During pulse off time debris and molten material efficiently flushed away and smoother surface results. Increase in pulse off time decreases the surface roughness.

### 4.5.3) Pulse on time (Pon)

From ANOVA results it is clear that Pon is the least significant factor with the percentage contribution of 8.83% in variation of surface roughness. The change in Pon value has negligible effect on surface roughness of Inconel 600. [19]

### 4.5.4) Wire Feed Rate (WFR)

From experimental data it is observed that WFR is the most significant factor with percentage contribution of 42.88%. Smaller changes in WFR can largely affect SR variation. ANOVA results shows p-value of WFR is less than  $\alpha$  (i.e 0.05), which shows its significance. At higher feed rates new wire came and improve surface finish quality. At higher feed rate minimum roughness can be achieved [20].

## 4.6) Optimal Process Parameters

Thus, the optimal setting of Inconel 600 for surface roughness through data means is found to be,

Table 4.11 Optimal process parameters for surface roughness.

Process Parameter	C (A)	Poff ( $\mu$ s)	Pon ( $\mu$ s)	WFR (m/min)
Optimal Setting	2	9	32	40

### 4.6.1) Confirmation Test Result

Confirmatory test is conducted to verify whether the optimal value of factors will achieve low kerf width. The model considered is adequate as results obtained from confirmatory test are satisfactory.

Table 4.12 Result of confirmation test for surface roughness

Response	Predicted Mean	Actual value	% Error
Surface Roughness	4.67667 $\mu$ m	5.03	7%

#### 4.7) XRD Analysis

XRD analysis of selected machined samples were done to check the characteristic peaks. Results are shown in Figure 4.3. There were no additional peaks observed in the graph, small peaks which may disappear during smoothing process or removing noise level from graph.

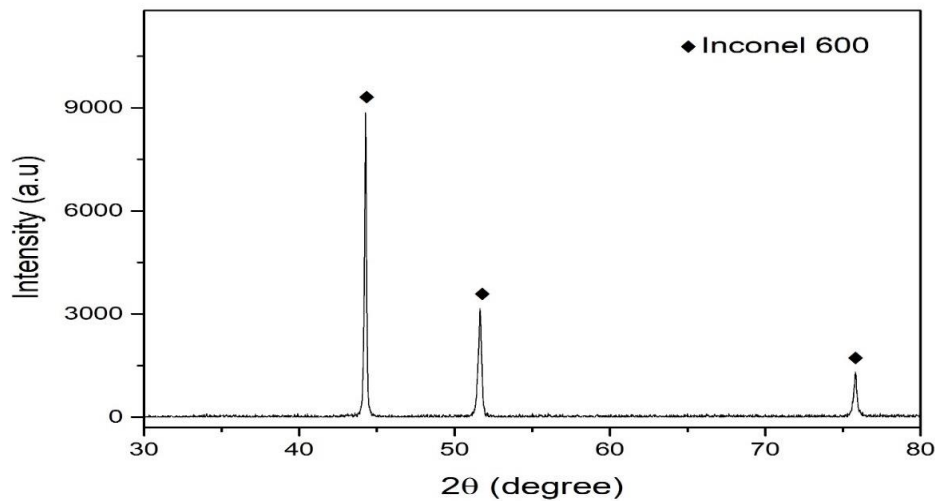


Figure 4.3 XRD plot for Inconel 600

#### 4.8) SEM Analysis for Grain Distortion Measurement

SEM analysis of various polished samples is conducted and grains distortion is measured using ImageJ software and listed in the table given below. The results indicate that intermediate values of current produce minimal grains distortion. Grain's distortion measured values against samples of Inconel 600 are given in table 4.13

Table 4.13 Grain's distortion measured values

S/No	Sampl e	C (A)	Poff ( $\mu$ s)	Pon ( $\mu$ s)	WFR (M/min)	SR (Ra)	Grain Distortion ( $\mu$ m)
1	In-1	1	5	32	20	7.91	24.56
2	In-6	2	9	32	30	5.32	9.6
3	In-8	3	7	32	40	5.03	21.67
4	In-9	3	9	64	20	6.80	27.635

Figure 4.6 shows the grain's distortion and measured results through ImageJ.

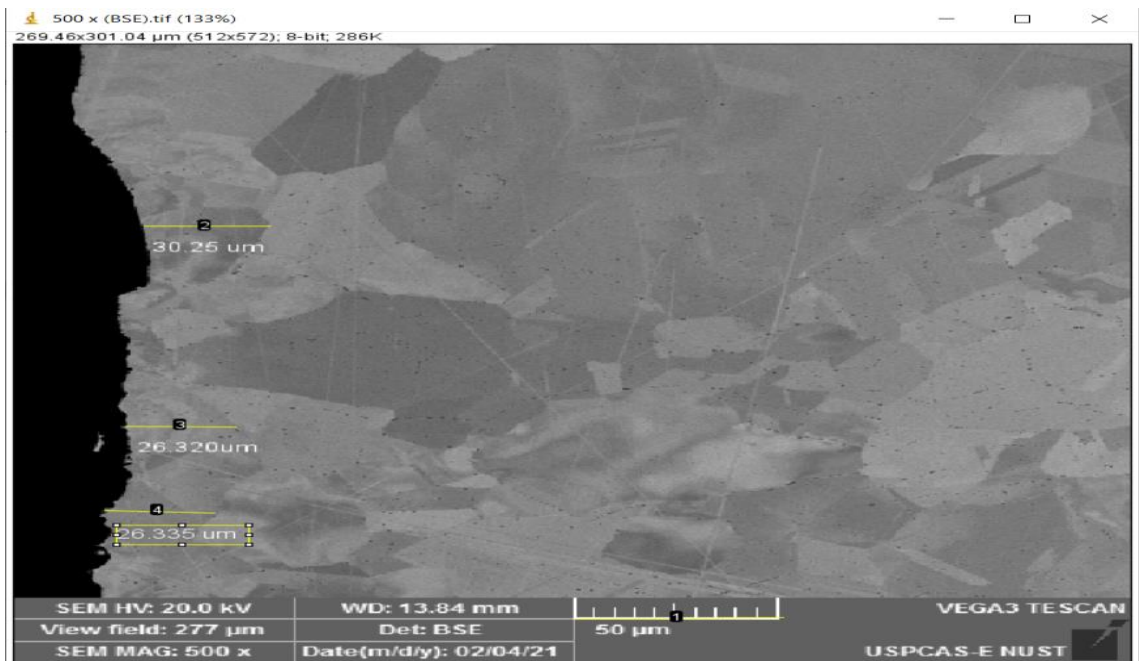


Figure 4.4 Grain distortion of machined surface

# CHAPTER 5

## Wire Electro Discharge Machining of Titanium Grade V

### Results and Analysis

In this chapter the kerf width and surface roughness results and findings for titanium grade V will be discussed and the effect of each factor on machine variables. Variance analysis is used to find out the significance of each machining parameter. To validate the result optimal values confirmatory test is conducted. Observations of experimental results are discussed below

#### 5.1) Kerf Width Results

Kerf width is the average of top and bottom kerf, top and bottom kerf width was measured through metallurgical microscope and using 5x lens as discussed in chapter 3. The measured kerf width values are given below in table 5.1

Table 5.1 Results for kerf width

S No	C	Poff	Pon	WFR	Kw
	Ampere	$\mu\text{s}$	$\mu\text{s}$	m/minute	$\mu\text{m}$
1	1	5	32	20	0.245030
2	1	7	64	30	0.271425
3	1	9	128	40	0.314335
4	2	5	64	40	0.340780
5	2	7	128	20	0.315265
6	2	9	32	30	0.276090
7	3	5	128	30	0.345650
8	3	7	32	40	0.339150
9	3	9	64	20	0.313395

### 5.1.1) Response Table for Data Means

Through analysis of variance input parameters effect on kerf width was studied and their ranking identified. The ranking of each parameter is shown in table 5.2

Table 5.2 Response table for mean kerf width

Level	C	Poff	Pon	WFR
1	11.198	10.264	10.929	10.773
2	10.185	10.249	10.252	10.578
3	9.566	10.436	9.769	9.598
Delta	1.632	0.188	1.160	1.175
Rank	1	4	3	2

### 5.1.2) Analysis of Variance

To calculate the contribution of each input parameter for kerf width ANOVA test is run for measured values of kerf width against each combination through MINTAAB 19. Significance of factors and their percentage contribution which is calculated is given in table 5.3

Table 5.3 Variance analysis for kerf width

Source	DF	Adj SS	Adj MS	Contribution	F-Value	P-Value	Significance
Regression	4	0.009282	0.002320		15.20	0.011	
C	1	0.004671	0.004671	47.61 %	30.60	0.005	Significant
Poff	1	0.000127	0.000127	0.7%	0.83	0.413	Not Significant
Pon	1	0.002061	0.002061	23.82 %	13.50	0.021	Significant
WFR	1	0.002423	0.002423	27.79%	15.88	0.016	Significant
Error	4	0.000611	0.000153				
Total	8	0.009892					

### 5.1.3) Regression Equation

Regression equation derived from ANOVA is given below showing the effect on kerf width

$$\text{Kerf Width} = 0.1785 + 0.02790 C - 0.00230 P_{off} + 0.000379 P_{on} + 0.002010 WFR$$

### 5.1.4) Model Summary

Model summary was tested at 95% confidence level and results shows that 87.66% variability of the data is explained by the considered model. Model summary results are shown in table 5.4

Table 5.4 Model summary for kerf width

S	R-sq	R-sq(adj)	R-sq(pred)
0.0123543	93.83%	87.66%	68.55%

### 5.1.6) Data Means Plot

In data means plot four factors (Peak current, pulse off time, pulse on time, wire feed rate) are used as input and response variable was surface roughness. The data means plot analysis basically used to check the effects of individual factor on response variable. Figure 5.2 shows the plot of input parameters and response variable.

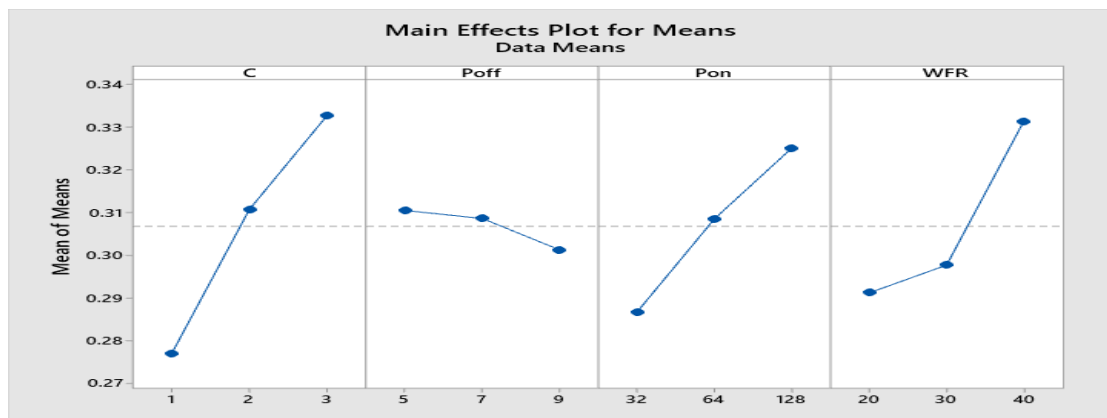


Figure 5.1 Main effect plots for data means for kerf width



## **5.2) Kerf Width Analysis**

The effect of each input parameter on kerf width of titanium grade V is discussed individually.

### **5.2.1) Peak current (C)**

Peak current observed the most dominant parameter for kerf width of titanium alloy. Its percentage contribution is 47.61%. It is observed that to minimize kerf width, it is desirable to use low peak current. At high peak currents large amount of discharge energy is available in cutting zone causing bigger kerf [21].

### **5.2.2) Pulse off time (Poff)**

Pulse off time has very low contribution towards the kerf width. However, its lower values are recommended to have minimum value of kerf width.

### **5.2.3) Pulse on time (Pon)**

The increase in kerf width is due to the attribution of higher discharge energy, high peak current and pulse on time increases the available discharge energy. That's why increasing trend can be observed for pulse on time and peak current.

### **5.2.4) Wire Feed Rate (WFR)**

As wire feed rate increased, there is less heat dissipation to the surrounding and more heat is generated at the spar gape leading to the bigger kerf width. Higher feed rates are not recommended as they lead to wire breaking phenomenon and produce higher inaccuracies.

## **5.3) Optimal Process Parameters**

Thus, the optimal setting of titanium grade V for kerf width are predicted from data means graphs and given below in table 5.5

Table 5.5 Optimal process parameters for kerf width

Process Parameter	C (A)	Poff ( $\mu$ s)	Pon ( $\mu$ s)	WFR (m/min)
Optimal Setting	1	9	32	20

### 5.3.1) Confirmation Test

Confirmation test was conducted on optimized parameters to minimize the kerf width. It was observed that the predicted and actual measured value of kerf width on optimized parameters is same and the system is adequate. Confirmation test results are shown in table 5.6

Table 5.6 Test results for kerf width

Response	Predicted Mean	Actual value	% Error
Kerf Width	0.235817	0.23506	0.32%

### 5.4) Surface Roughness Results

Surface roughness is one of the important output responses, which is desired to be minimized for the machined samples. Surface roughness of the all-machined samples of titanium grade V is measured and average value of surface roughness is given below in table 5.7

Table 5.7 Results for surface roughness

S No	C	Poff	Pon	WFR	SR Mean (Ra)
	Ampere	$\mu\text{s}$	$\mu\text{s}$	m/minute	$\mu\text{m}$
1	1	5	32	20	8.65
2	1	7	64	30	7.58
3	1	9	128	40	6.41
4	2	5	64	40	5.53
5	2	7	128	20	5.98
6	2	9	32	30	4.59
7	3	5	128	30	6.94
8	3	7	32	40	5.03
9	3	9	64	20	5.95

#### 5.4.1) Response Table for Data Means

Variance analysis is use to check the ranking of each parameter. From the above given data of surface roughness, ranking of all input parameters is calculated and given in the table 5.8

Table 5.8 Response table for mean surface roughness

Level	C	Poff	Pon	WFR
1	7.547	7.040	6.090	6.860
2	5.367	6.197	6.353	6.370
3	5.973	5.650	6.443	5.657
Delta	2.180	1.390	0.353	1.203
Rank	1	2	4	3

#### 5.4.2) Analysis of Variance

Results derived from ANOVA are used to calculate the percentage contribution of each variable and through p-value parameters significance is predicted. ANOVA results for percentage contribution and significance of factors are given in table 5.9

Table 5.9 Variance analysis for surface roughness

Source	DF	Adj SS	Adj MS	Contribution	F-Value	P-Value	Significance
Regression	4	8.9447	2.2362		2.24	0.227	
C	1	3.7131	3.7131	57.52 %	3.72	0.126	Not Significant
Poff	1	2.8982	2.8982	21.86 %	2.90	0.164	Not Significant
Pon	1	0.1614	0.1614	4.7 %	0.16	0.708	No Significant
WFR	1	2.1720	2.1720	15.81%	2.18	0.214	Not significant
Error	4	3.9926	0.9981				
Total	8	12.9372					

### 5.4.3) Regression Equation

Regression equations is obtained for surface roughness after analyzing the impact of all Individual parameters, providing a good relationship between machining parameters and Output parameters.

$$\text{Surface Roughness} = 11.86 - 0.787C - 0.348 \text{ Poff} + 0.00336 \text{ Pon} - 0.0602 \text{ WFR}$$

### 5.4.4) Model Summary

Model summary was tested at 95% confidence level. The results shows that 38.16% variability of the data is explained by the considered model. Model summary results are shown in table 5.10

Table 5.10 Model summary for surface roughness

S	R-sq	R-sq(adj)	R-sq(pred)
0.999070	69.14%	38.28%	0.00%

### 5.4.6) Main Effect Plot for Data Means

Individual variable response against surface roughness was plotted graphically, which shows the effect of each input parameter level on the surface roughness of WEDM machined samples. Data means plot for surface roughness is shown in figure 5.2

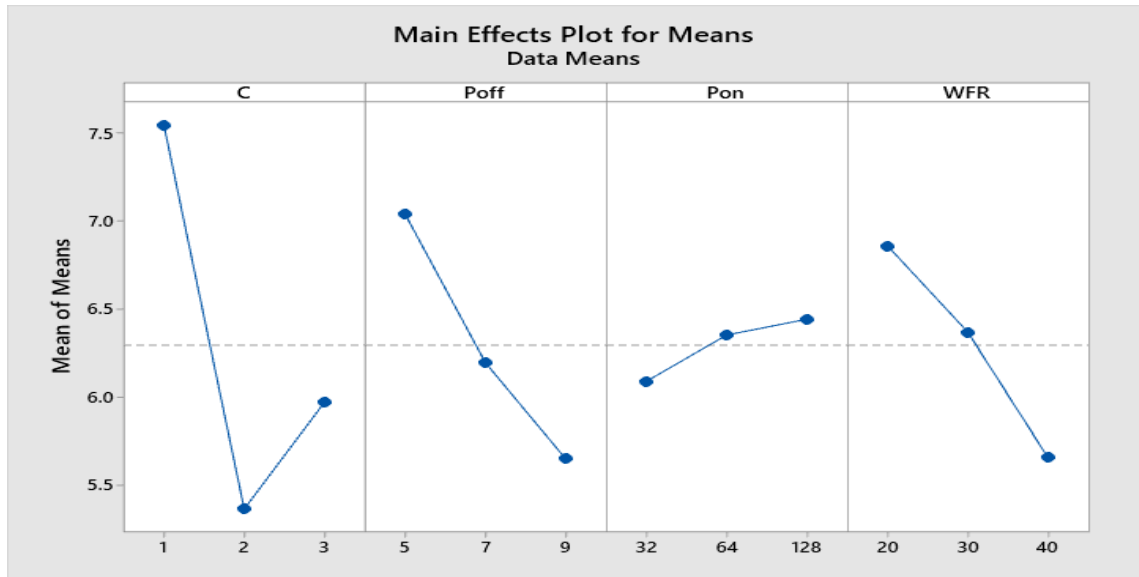


Figure 5.2 Main effect plot for data means for surface roughness

## 5.5) Surface Roughness Analysis

Effect of each input parameter on the surface roughness is discussed below

### 5.5.1) Peak Current (C)

Intermediate values of peak current are recommended for lower surface roughness. Larger peak currents produce bigger crater due to high discharge energy available between the spark gap and eroding more material [18].

### 5.5.2) Pulse off time (Poff)

During pulse off time dielectric fluid flushed away the molten material between the spark gap and produce smoother surface. Higher pulse off time setting is desirable for producing less rough surfaces.

### 5.5.3) Pulse on time (Pon)

Least contribution of pulse on time was observed for surface roughness of machined samples. From ANOVA results it is clearly shown Pon has least contribution in variation of surface roughness[19].

### 5.5.4) Wire feed rate (WFR)

When wire feed rate increases surface roughness decreasing trend observed. As the wire feed rate increases new wire came and improvement in surface finish occur that means surface roughness decreases with increase in wire feed rate [20].

## 5.6) Optimal Process Parameters

Surface roughness should be minimized for the process and for this purpose process parameters are optimized. Optimal parameters machine settings are given in table 5.11

Table 5.11 Optimal process parameters for surface roughness

Process Parameter	C (A)	Poff ( $\mu$ s)	Pon ( $\mu$ s)	WFR (m/min)
Optimal Setting	2	9	32	40

### 5.6.1) Confirmation Test Result

Confirmation test was conducted on optimized parameters to minimize the surface roughness. It was observed that the predicted and actual measured value of surface roughness on optimized parameters for titanium grade V is not same. This is due to poor thermal conductivity of titanium alloy. Confirmation test results are shown in table 5.12

Table 5.12 Test results for surface roughness

Response	Predicted Mean	Actual value	% Error
Surface Roughness	3.87667 $\mu$ m	16.07	75%

### 5.7) XRD Analysis

XRD analysis of selected machined samples were done to check the characteristic peaks of elements and compounds. Titanium, Aluminum and Titanium oxide peaks with their card number are shown below in figure 5.3

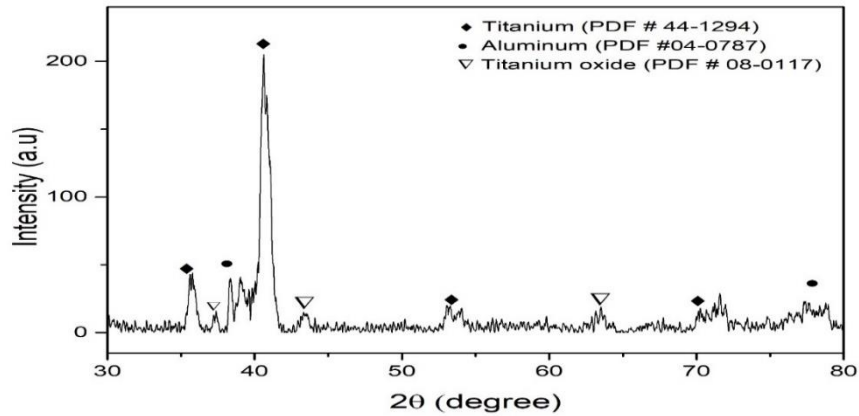


Figure 5.3 XRD graph for Titanium grade 5

### 5.8) SEM Analysis for Grain Distortion Measurement

Grains distortion of image obtained from SEM analysis is measured through imageJ software and shown in figure 5.4

Table 5.13 Grain's distortion result

S/No	Sample	C (A)	Poff (μs)	Pon (μs)	WFR (M/min)	SR (Ra)	Grain Distortion (μm)
1	T-9	3	9	64	20	6.80	22.0345

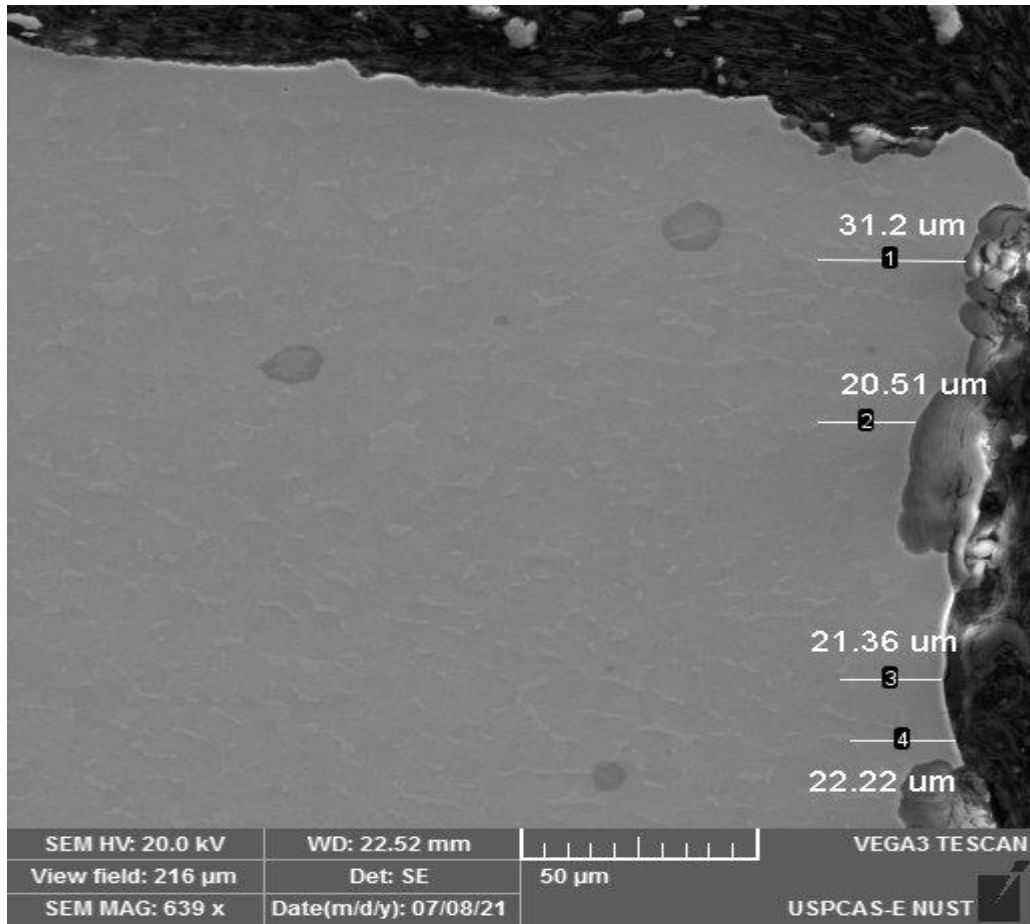


Figure 5.4. Titanium Sample 9 grains distortion



# CHAPTER 6

## CONCLUSIONS AND RECOMMENDATIONS

### 6.1) Conclusions

In this present experimental work parametric analysis of Titanium grade V and Inconel 600 is done using wire electrical discharge cutting technique. Optimization of surface roughness and kerf width is done using Taguchi methodology. Geometrical study of grain distortion is carried out using SEM analysis. XRD analysis is used to identify the characteristic peaks of elements and compounds.

Following conclusions have been drawn after analysis:

#### INCONEL 600

- For kerf width pulse on time and peak current are most significant factors with contribution of 39.40% and 22.69 % respectively.
- Kerf width can be minimized using short pulse on time and low peak current, but increases the production cost.
- Wire feed rate is the most influential factor affecting surface roughness with contribution of 42.88 % while peak current is marked as sub significant.
- T obtaining smooth surface, high wire feed rates and intermediate of peak current should be preferred.
- Grain distortion results are relatable to surface roughness trends. At intermediate peak current values lower grain distortion is observed.

#### TITANIUM GRADE V

- For kerf width peak current plays a major role with contribution of 47.61 %.
- Kerf width can be minimized at low peak current at the cost of production rate.
- For surface roughness peak current and pulse off time are the most influential factors with contribution of 57.52 % and 21.86 % respectively.

- For obtaining smooth surface, intermediate peak current and high pulse off time should be preferred.
- Grain distortion increases with increase in peak current, intermediate values of peak current levels exhibit smaller grain distortion.

## **6.2) Recommendations**

- Optimization of grain distortion using Taguchi methodology to identify significant input parameters and their %age contribution

# REFERENCES

- [1] S. H. I. Jaffery and P. T. Mativenga, "Wear mechanisms analysis for turning Ti-6Al-4V-towards the development of suitable tool coatings," *Int. J. Adv. Manuf. Technol.*, vol. 58, no. 5–8, pp. 479–493, Jan. 2012, doi: 10.1007/s00170-011-3427-y.
- [2] X. Liang, Z. Liu, and B. Wang, "State-of-the-art of surface integrity induced by tool wear effects in machining process of titanium and nickel alloys: A review," *Measurement: Journal of the International Measurement Confederation*, vol. 132. Elsevier B.V., pp. 150–181, Jan. 01, 2019, doi: 10.1016/j.measurement.2018.09.045.
- [3] M. Sreenivasa Rao and N. Venkaiah, "Experimental investigations on surface integrity issues of Inconel-690 during wire-cut electrical discharge machining process," *Proc. Inst. Mech. Eng. Part B J. Eng. Manuf.*, vol. 232, no. 4, pp. 731–741, Mar. 2018, doi: 10.1177/0954405416654092.
- [4] J. Kapoor, S. Singh, and J. S. Khamba, "High-performance wire electrodes for wire electrical-discharge machining - A review," *Proceedings of the Institution of Mechanical Engineers, Part B: Journal of Engineering Manufacture*, vol. 226, no. 11. pp. 1757–1773, Nov. 2012, doi: 10.1177/0954405412460354.
- [5] F. Han, J. Jiang, and D. Yu, "Influence of discharge current on machined surfaces by thermo-analysis in finish cut of WEDM," *Int. J. Mach. Tools Manuf.*, vol. 47, no. 7–8, pp. 1187–1196, Jun. 2007, doi: 10.1016/j.ijmachtools.2006.08.024.
- [6] B. Gugulothu, "Optimization of process parameters on EDM of titanium alloy," in *Materials Today: Proceedings*, Jan. 2020, vol. 27, pp. 257–262, doi: 10.1016/j.matpr.2019.10.150.
- [7] A. Okada, Y. Uno, S. Onoda, and S. Habib, "Computational fluid dynamics analysis of working fluid flow and debris movement in wire EDMed kerf," *CIRP Ann. - Manuf. Technol.*, vol. 58, no. 1, pp. 209–212, 2009, doi: 10.1016/j.cirp.2009.03.003.
- [8] W. : Www, J. R. Mevada, C. D. Shah, and B. C. Khatri, "International Journal of Emerging Technology and Advanced Engineering A Wear Investigation of Repeatedly Used Wire in

- Wire Cut Electrical Discharge Machine,” 2008. [Online]. Available: [www.ijetae.com](http://www.ijetae.com).
- [9] M. Garg, G. Bhushan, and A. Jain, “An Investigation into Dimensional Deviation Induced by Wire Electric Discharge Machining of High temperature Titanium alloy,” *J. Eng. Technol.*, vol. 2, no. 2, p. 104, 2012, doi: 10.4103/0976-8580.99298.
- [10] A. Shah, N. A. Mufti, D. Rakwal, and E. Bamberg, “Material removal rate, kerf, and surface roughness of tungsten carbide machined with wire electrical discharge machining,” *J. Mater. Eng. Perform.*, vol. 20, no. 1, pp. 71–76, Feb. 2011, doi: 10.1007/s11665-010-9644-y.
- [11] S. Kumar, S. Dhanabalan, and C. S. Narayanan, “Application of ANFIS and GRA for multi-objective optimization of optimal wire-EDM parameters while machining Ti–6Al–4V alloy,” *SN Appl. Sci.*, vol. 1, no. 4, Apr. 2019, doi: 10.1007/s42452-019-0195-z.
- [12] A. Kumar, U. A. Kumar, and P. Laxminarayana, “Optimization of surface roughness and kerf width by wire cut-electrical discharge machining on inconel 625,” in *Materials Today: Proceedings*, Jan. 2020, vol. 27, pp. 1460–1465, doi: 10.1016/j.matpr.2020.02.955.
- [13] K. Manikandan, P. Ranjith kumar, D. Raj kumar, and K. Palanikumar, “Machinability evaluation and comparison of Incoloy 825, Inconel 603 XL, Monel K400 and Inconel 600 super alloys in wire electrical discharge machining,” *J. Mater. Res. Technol.*, vol. 9, no. 6, pp. 12260–12272, 2020, doi: 10.1016/j.jmrt.2020.08.049.
- [14] K. Muralova, J. Kovar, L. Klakurkova, and T. Prokes, “Effect of Width of Kerf on Machining Accuracy and Subsurface Layer After WEDM,” *J. Mater. Eng. Perform.*, vol. 27, no. 4, pp. 1908–1916, Apr. 2018, doi: 10.1007/s11665-018-3239-4.
- [15] A. Kumar, S. Dhanabalan, S. Kumar, V. Kumar, and J. Kumar, “Prediction of Surface Roughness in Wire Electric Discharge Machining (WEDM) Process based on Response Surface Me... Prediction of Surface Roughness in Wire Electric Discharge Machining (WEDM) Process based on Response Surface Methodology,” *Int. J. Eng. Technol.*, vol. 2, no. 4, 2012.
- [16] S. P. Arikatla, T. Mannan, and A. Krishnaiah, “Engineering and Technology (A High Impact

- Factor," *Int. J. Innov. Res. Sci.*, vol. 5, no. 1, 2016, doi: 10.15680/IJIRSET.2015.0501034.
- [17] E. & Abele and B. Fröhlich, "HIGH SPEED MILLING OF TITANIUM ALLOYS," *Adv. Prod. Eng. Manag.*, vol. 3, pp. 131–140, 2008.
- [18] Y. Nawaz, S. Maqsood, K. Naeem, R. Nawaz, M. Omair, and T. Habib, "Parametric optimization of material removal rate, surface roughness, and kerf width in high-speed wire electric discharge machining (HS-WEDM) of DC53 die steel," *Int. J. Adv. Manuf. Technol.*, vol. 107, no. 7–8, pp. 3231–3245, 2020, doi: 10.1007/s00170-020-05175-3.
- [19] U. M. R. Paturi, S. Cheruku, V. P. K. Pasunuri, S. Salike, N. S. Reddy, and S. Cheruku, "Machine learning and statistical approach in modeling and optimization of surface roughness in wire electrical discharge machining," *Mach. Learn. with Appl.*, vol. 6, no. June, p. 100099, 2021, doi: 10.1016/j.mlwa.2021.100099.
- [20] V. Sharma and U. Viyat Varun, "A Review on: Effect of controllable factor on Material removal rate and surface roughness during WEDM," *IOP Conf. Ser. Mater. Sci. Eng.*, vol. 1116, no. 1, p. 012093, 2021, doi: 10.1088/1757-899x/1116/1/012093.
- [21] S. Tilekar, S. S. Das, and P. K. Patowari, "Process Parameter Optimization of Wire EDM on Aluminum and Mild Steel by Using Taguchi Method," *Procedia Mater. Sci.*, vol. 5, pp. 2577–2584, 2014, doi: 10.1016/j.mspro.2014.07.518.